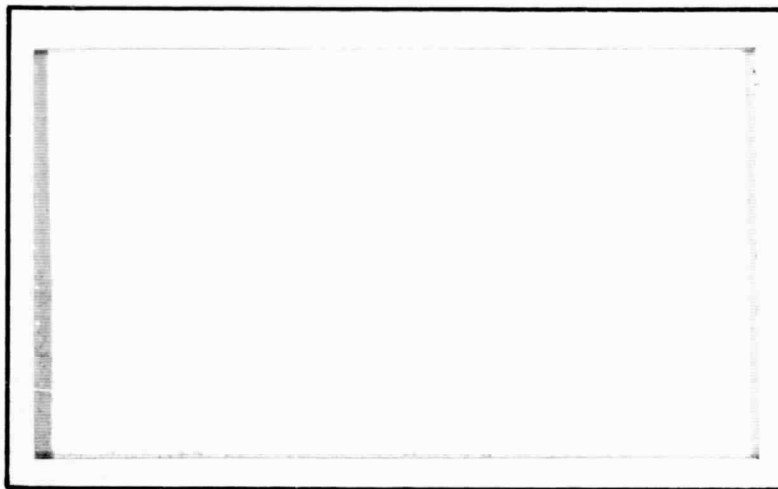


General Disclaimer

One or more of the Following Statements may affect this Document

- This document has been reproduced from the best copy furnished by the organizational source. It is being released in the interest of making available as much information as possible.
- This document may contain data, which exceeds the sheet parameters. It was furnished in this condition by the organizational source and is the best copy available.
- This document may contain tone-on-tone or color graphs, charts and/or pictures, which have been reproduced in black and white.
- This document is paginated as submitted by the original source.
- Portions of this document are not fully legible due to the historical nature of some of the material. However, it is the best reproduction available from the original submission.



FACILITY FORM 502

N68 37604

(ACCESSION NUMBER)

74

(PAGES)

CR-98042

(NASA CR OR TMX OR AD NUMBER)

(THRU)

(CODE)

13
(CATEGORY)



FAIRCHILD HILLER

REPUBLIC AVIATION DIVISION

FARMINGDALE, LONG ISLAND, NEW YORK

GPO PRICE \$ _____

CFSTI PRICE(S) \$ _____

Hard copy (HC) 3.00

Microfiche (MF) 65

ff 653 July 65



PCD-TR-67-9
FHR 3287-1
PC090R0001
September, 1967

FINAL REPORT
Volume I - Summary Technical Report

**Measurement of Electric Fields
In The Ionosphere**

For Period: August, 1966 - September, 1967

Contract NAS 8-20663

September, 1967

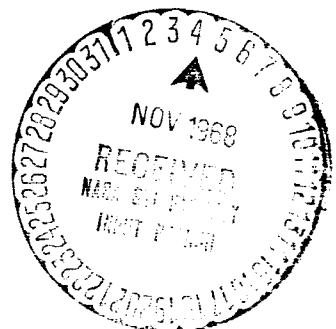
by

**Gerald Levy
Herbert Jacobs
Edgar Tendor**

Prepared For:

**George C. Marshall Space Flight Center
National Aeronautics and Space Administration
Huntsville, Alabama 35812**

**FAIRCHILD HILLER CORPORATION
Republic Aviation Division
Power Conversion Department
Farmingdale, New York 11735**



CONTENTS

<u>SECTION</u>		<u>PAGE</u>
	FOREWORD	iii
	ABSTRACT	iv
	NOTATIONS	v
I	INTRODUCTION	1
	A. General	1
	B. Electric Field Measurements within the Ionosphere	2
	C. History of Development	5
II	THEORETICAL ANALYSIS	7
	A. Introduction	7
	B. Ionospheric Conditions	7
	C. Mathematical Fundamentals	8
	D. Regions of Interaction-Qualitative Considerations	9
	E. The Far Field - Region A	11
	F. The Surface Potential	12
	G. The Upstream Near Field	13
	H. Downstream Near Field	14
	I. Upstream Debye Region	16
	J. The Downstream Debye Region	17
	K. Conclusions	18
III	INSTRUMENT DESIGN AND PERFORMANCE	21
	A. Concepts	21
	B. Component Description	24
	C. Environment	30
	D. Laboratory Test Procedure	31
	E. Laboratory Performance	32
IV	MISSION CONSIDERATIONS	37
	A. Mission Categories	37
	B. Mission Concepts	38
	C. Meter Constraints	43
	D. Attitude Resolution Requirements	48
	E. Mission Configurations	56
	F. In-Flight Electric Field Meter Operation	64
	References	67

FOREWORD

This report describes the development of an experimental laboratory model of an electric field meter using the electron beam deflection technique and the system considerations for its use. This meter is designed to operate within the ionosphere in the vicinity of spacecrafts.

The effort was supported by the Space Science Laboratory of George C. Marshall Space Flight Center under the technical management of Mr. E. L. Shriver with the consultation of Dr. A. H. Weber, Chairman of the Physics Department of St. Louis University.

The facilities of Republic Aviation Division of Fairchild Hiller Corporation, Power Conversion Department which is under the direction of Mr. A. E. Kunen, were made available for this work.

The project investigator was Mr. G. Levy. The chief instrument engineer was Mr. H. Jacobs and principal physicist was Dr. E. Bendor. Major contributions to the program were made by Dr. L. Zadoff, Mr. S. Cohen, and Mr. E. Kuhn. The assistance of Mr. P. Forsyth and Mr. E. Vogel in establishing the framework of the problem is gratefully acknowledged. Messrs: G. Stewart, C. Hausman, and L. Brown very capably provided the technical support in the laboratory.

This work was performed under contract number NAS 8-20663. The Final Report, Volume I, "Summary Report", is Fairchild Hiller Corporation Report No. PCD-TR-67-9, FHR 3287-1, dated September, 1967.

ABSTRACT

The measurement of electric fields within the ionosphere is complicated by the highly ionized media, the Earth's magnetic field, and the relative motion of the instrument with respect to the ionosphere. A sensitive electric field meter which has a five order of magnitude dynamic range has been developed for use within the ionosphere and has been laboratory tested.

The meter utilizes the technique of the deflection of an electron beam under the influence of the electric field to be measured. Since the velocity of the beam relative to the Earth's magnetic field produces a significant deflection, the electric field being measured is chopped by the intermittent operation of a Faraday cage. This separates to two fields deflecting the beam thereby increasing the sensitivity and range of the instrument. The deflection of the beam is monitored on a segmented target. Displacements as small as 10^{-5} mm are detected. The deflection signal is amplified and fed back to the deflection plates to continually null the virtual center of the beam. Two components of the electric field orthogonal to the beam direction are simultaneously measured. The output of the loop is synchronously detected and filtered. Thus a d.c. voltage level which is proportional to the electric field being measured is available for read-out.

The meter is designed to operate within the ionosphere and to measure electric fields from 10 mv/meter to 1000 volts/meter with a sensitivity of ± 1 mv/meter at 10 mv/meter, and $\pm 1\%$ above 100 millivolt/meter.

Ambient electric fields within the ionosphere have been measured to range from 10 millivolt/meter and less, up to 100 millivolt/meter and more. While electric fields near surfaces of spacecraft and probes surrounded by a plasma sheath can range up to 1000 volts/meter. Thus a versatile meter for use in ionospheric measurements of electric fields associated with the spacecraft must have a wide dynamic range and be extremely sensitive. The design analysis included plasma sheath and wake effects of the meter components and nearby bodies, the modification of the ambient electric field and plasma properties due to the electron beam, and the attitude resolution requirements to determine the apparent electric field due to the $(\vec{v} \times \vec{B})$ of the spacecraft and magnetosphere which is inseparable from all electric field measurements.

Conceptual configurations of experiments that could utilize the AAP Workshop or a sounding rocket are also presented in this report.

NOTATIONS

c	Velocity of light	
d	Body dimension	
e	Electronic charge	
\underline{E}, E	Electric field	
f	Distribution function	
H	Magnetic field	
j	Current density	
k	Boltzmann's constant	
l	Larmor radius	
m	Particle mass	
\underline{r}	Position vector	
n	Particle density	
R	Reflection factor	
S_{∞}	"Speed ratio" $(m_e v^2/2kT)^{1/2}$	
T	Temperature	
u	Random velocity	
\underline{V}, V	Vehicle velocity	
δ_{∞}	Debye length based on n_{∞} as $(kT/4\pi e^2 n_{\infty})^{1/2}$	
ξ, η	Distances, parallel and normal to the beam path	
θ, φ	Angles	
t	Time	
λ	Mean free path	
ν	Collision frequency	
Φ	Electric potential	O() of the order of

SUFFIXES

s	Surface
∞	At infinity
e	Electrons
i	Ions
r	After reflection
b	Satellite body
f	Field meter components
th	Thermal
coll	Collisions

SECTION I

INTRODUCTION

A. GENERAL

The measurement of electric fields in the vicinity of spacecraft operating within the ionosphere has presented many problems. The paucity of knowledge of electric fields within the ionosphere is a reflection of the extreme difficulty in obtaining this information without modifying the fields being measured. ⁽¹⁾

In addition to the scientific requirement of understanding the space environment, there are also engineering requirements which necessitate the development of an electric field meter which is compact, can operate within the ionosphere, has a wide dynamic range and is extremely sensitive to small field changes. These engineering requirements include the measurement of:

- (1) Electric fields created by charged particulate clouds near the spacecraft.
- (2) Electric fields created by the plasma sheath surrounding the spacecraft.
- (3) Electrodynamic forces and moments upon the spacecraft caused by this charged body moving through an ambient ionospheric electric field.

A meter that fulfills these requirements must be relatively compact so that it can be moved from point to point within the spacecraft's external environment without elaborate calibration or mechanical requirements. The range of electric fields that this meter encounters will vary from 1000 volts/meter close to the vehicle surface down to 10 millivolts/meter at a distance of 5 body radii from the spacecraft, thus a meter used for housekeeping of the environment needs a wide dynamic range. The meter should not modify the electric field or other environment parameters, in particular, the field sensing element should be a non-participating observer. The physical construction of the meter must consider the plasma properties of the ionosphere-magnetosphere in relation to a body moving through it.

This report describes the development of an electron beam electric field meter which has been designed to perform these engineering tasks as well as the survey of the ambient electric field within the ionosphere.

B. ELECTRIC FIELD MEASUREMENTS WITHIN THE IONOSPHERE

The measurement of the electric field in the vicinity of the spacecraft within the ionosphere presents many unique problems in meter design and interpretation of data.

Electric fields in the atmosphere or vacuums are commonly measured by "field mills". These meters measure the charge collected on a metal surface which is intermittently screened from the field to be measured.⁽²⁾ Another means is by the potential difference of two or more high impedance probes of known geometry.⁽³⁾ In addition charged particle interaction with the field to be measured has also been used.⁽⁴⁾ Two of the most severe problems associated with the measurement of electric fields within the ionosphere are:

- 1) The ionosphere consists of a highly ionized plasma. A plasma sheath develops about bodies which produce high electric fields near surfaces. The conductivity of the plasma tends to neutralize charges collected by the meters.
- 2) Vehicle motion relative to the earth's magnetic field produces an apparent electric field which must be known in order to determine the actual electric field being measured.

The "field mill" class of meters are thus faced with the problems that the plasma sheath covering the meter creates electric fields, as high as 1000 volts/meter, at the surfaces used for charge collection. Also electric currents flow from the plasma to the field mill. Since the concept of this meter is the measurement of current flowing to a surface element that is intermittently screened from the outer field, it is noted that the sensing element in a plasma presents extreme difficulties to the measurement of electric fields.

The electrostatic potential difference probes are faced with similar difficulties. Each probe of the measuring system is surrounded by a plasma sheath and acquires a potential different from the plasma. The voltage drop in a sheath depends upon the geometry and orientation of the probes; thus the potential difference may not be the same for each probe. The orientation of the probes is extremely important since, due to the earth's magnetic field, the plasma is anisotropic. Further, the probes must be far away from each other and all other obstacles that could disturb the symmetry by screening different parts of the incoming charged particle flux. In addition, the probe material and electrical connections must be identical physically and electrically to assure the same photoemission and electrical impedance characteristics. The distance between the probes becomes extremely great when small fields are being measured. For example, Fahleson⁽⁵⁾ has performed an excellent design evaluation for the measurement of electric fields in the ionosphere using a probe system; he finds that a 300 km altitude minimum probe distance of 6 meters must be used to assure all the design restraints are met. For higher altitude, the distance becomes significantly greater. This analysis assumed that the meter constituted the spacecraft; if the meter was carried aboard a multipurpose spacecraft, it would have to be placed at an extremely large distance from the craft to assure no screening that would destroy the symmetry.

Another technique that is being used to measure the electric fields in the ionosphere is the motion of an ionized barium cloud. In these experiments barium vapor is released at altitude in sunlight. The cloud is rapidly photoionized (within 100 seconds) and is diffused in a long straight beam in the earth's magnetic field. The relative motion of this barium cloud and a neutral gas cloud simultaneously released is used to determine the electric field in the ionosphere. The increased ionization caused by the presence of the ionized cloud within the ionosphere modified the ambient electric field, and the diffusion of the magnetic field into the ionized gas cloud creates a time as well as a spatially dependent problem which is still being analyzed.

In summary, the only compact (quasi-point) field measuring device presently being used is the field mill, however, significant problems are associated with its

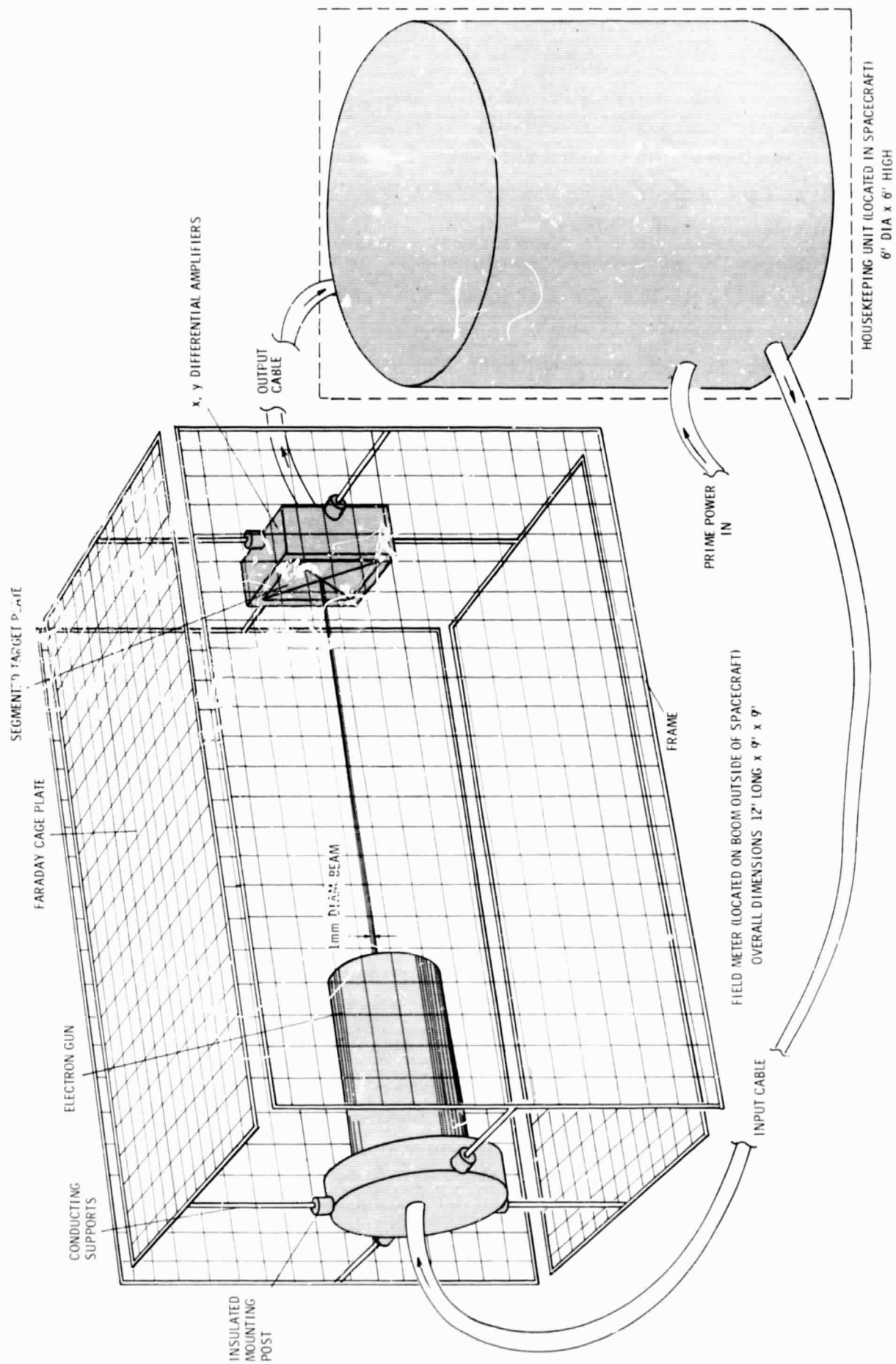


Figure 1: Electron Beam Deflection Electric Field Meter

use in the highly ionized ionosphere. The potential probe systems and barium cloud techniques are applicable over large spatially separated points or volumes remote from the spacecraft. None of these concepts meet the requirement for an electric field meter that can measure electric fields in the vicinity of a spacecraft within the ionosphere.

The electron beam electric field meter has been designed to meet this requirement. This meter utilizes the deflection of an electron beam under the influence of an electric field. The sensitivity of the device is enhanced by utilizing a feed-back loop which continually nulls the virtual center of the electron beam and by synchronously detecting chopped electric field deflections. The meter is designed to operate within the ionosphere and has a range from 10 millivolts/meter to 1000 volts/meter. It has a sensitivity of ± 1 millivolt/meter at the 10 mV/meter level. The meter that will be designed for space use will have a physical size of 1 foot long by 9 inches on the sides and weigh under 1 pound, and the auxiliary housekeeping package will be remote from the meter, weighing 2 pounds and occupying a volume of 0.1 cubic feet. These units are shown in Figure 1.

C. HISTORY OF DEVELOPMENT

In 1964, the Marshall Space Flight Center's Space Sciences Laboratory began an in-the-house investigation of the use of electron beam deflection to measure electric field strength. The results of this feasibility study and associated laboratory effort demonstrated that fields of less than 1 volt/meter could easily be measured in the laboratory.⁽⁶⁾

The present work described in this report is the development of an experimental laboratory model of an electric field meter using the electron beam deflection technique and the system considerations for its use. This meter is designed to operate in the vicinity of a spacecraft within the ionosphere. The use of a weak electron beam (less than 1 microampere) provides a field sensing element which does not disturb the environment or the field it is measuring, while still permitting the association of the measured fields with the orbiting spacecraft at desired locations on, near, or far from its surface.

SECTION II

THEORETICAL ANALYSIS

A. INTRODUCTION

In the theoretical aspects of the present work on electron beam field meters we have been concerned mainly with the electric fields induced by bodies moving in the ionosphere. By "bodies", in this context, we mean not only satellite vehicles (with metallic or dielectric surfaces) and their extensions, but also components of the field meter itself. The magnitude and details of the electrostatic potential induced in the neighborhood of such bodies are functions of the properties of the surface, the state of the ionospheric plasma, the ambient velocity and electric field vectors, etc. In certain circumstances the induced field may be much larger than the field which it is intended to measure, so that care must be taken in the use of the field meter and the interpretation of the data obtained therewith. It is the purpose of the theoretical work described below to reveal what the order of magnitude of this particular source of "noise" will be under various conditions of use and orientations of the instrument.

B. IONOSPHERIC CONDITIONS

We shall be interested in the ionosphere above 200 km altitude (the E & F regions). The conditions prevailing here, briefly stated, are the following: The percentage ionization is low, varying from approximately 10^{-3} % at 200 km to about 10% at 700 km. The temperature is between 1000°K and 2000°K for ions and neutrals; the electron temperature would be higher nearer the top of the ionosphere due to the high energy tail in the electron distribution which, however, we shall not take into consideration. The mean free path of electrons, ions, and neutrals is very large compared with the vehicle dimensions so that we shall be dealing with the electrons and ions without reference to their neutral background except for the single instance of the anisotropy due to an ambient field (see para. E). We have made no mention of the interaction between neutral particles and the vehicle, a subject which is adequately dealt with elsewhere and will not in any case concern us unless we are interested in vehicle drag.

As mentioned above we are concerned with two distinct kinds of bodies; the vehicle and the field meter components, the latter being taken as two orders of magnitude smaller than the former. The Larmor radius of electrons is a few centimeters and therefore of the order of the dimensions of the field meter components; the Larmor radius of ions is of the order of magnitude of the dimensions of a typical satellite vehicle. (Of course, the Larmor radius depends on the location in the magnetosphere, but the above are typical values). The Debye radius based on the ambient electron density varies between 0.1 cm and 1 cm depending upon the altitude and ambient conditions. Finally, the ratios: $|v_{i \text{ thermal}}|/V$ and $|v_{e \text{ thermal}}|/V$ are of the greatest importance in the analysis and we shall have a cause to refer frequently to the fact that the former is small and the latter is large. In other words, the kinetic energy of ions is much greater than their thermal energy whereas the kinetic energy of electrons is much smaller than the thermal energy. Finally, since one of the principal applications of the field meter will be to the measurement of the ambient electric field (E_∞) we should know the order of magnitude of this field, as quoted from experimental data, (Gdalevich and Imyanitov⁽¹¹⁾). This field is of the order of 10^{-2} v/meter to 10^{-1} v/meter, its orientation being perpendicular to the local geomagnetic field vector. The field parallel to the magnetic field lines is at least two orders of magnitude less. This orientation arises of course from the manner in which E_∞ is created (ionospheric plasma flowing across the geomagnetic field).

C. MATHEMATICAL FUNDAMENTALS

The underlying equations in the various problems considered below are the Boltzmann equation for electrons and the Poisson equation for the potential:

$$\underline{v} \cdot \frac{\partial f_e}{\partial \underline{r}} + \frac{e}{m_e} \left\{ - \frac{\partial \Phi}{\partial \underline{r}} + \frac{1}{c} (\underline{v} + \underline{V}) \times \underline{H} \right\} \cdot \frac{\partial f_e}{\partial \underline{v}} = \left(\frac{\partial f_e}{\partial t} \right)_{\text{coll.}} \quad (1)$$

$$\nabla^2 \Phi = -4\pi e \left\{ n_i(\underline{r}) - \int f_e d\underline{v} \right\} \quad (2)$$

As we shall see, the Boltzmann equation for ions can be avoided at least to a first order, since the influence of the potential field on the motion of ions can be shown to be small. It is only when this perturbation to the assumed conditions is to be investigated that it becomes necessary to consider the ion distribution function.

In addition to these two fundamental equations we have to satisfy the condition that the total current flowing into the surface is zero:

$$\underline{j}_i \cdot \underline{n} = \int_{\text{surface}} e f_e (\underline{v} \cdot \underline{n}) dv \quad (3)$$

This condition has to be satisfied locally on a dielectric surface; for a conductor it is sufficient that the total current flowing into the whole surface shall be zero.

We have neglected here the effects of thermionic or photoelectric emission and artificial currents such as those due to electrical engines, etc. We shall deal with these equations in a frame fixed in the vehicle. The Maxwellian distribution is therefore:

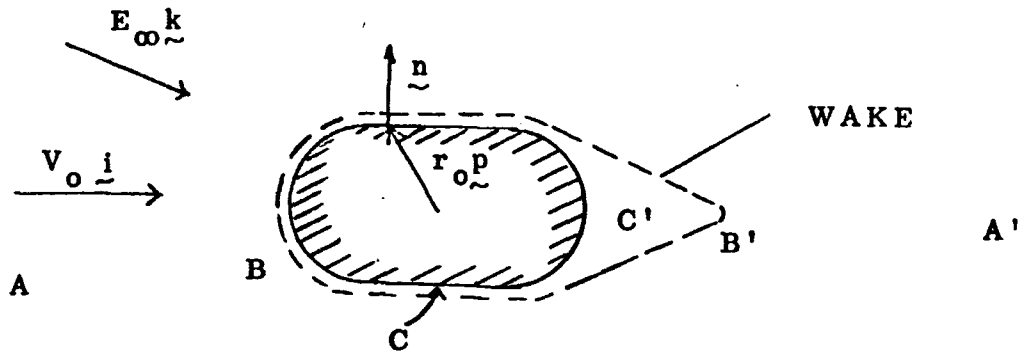
$$f = n_{\infty} \left(\frac{m}{2\pi kT} \right)^{3/2} \exp \left\{ -\frac{m}{2kT} (\underline{v} + \underline{V})^2 \right\} \quad (4)$$

This distribution applies for the ions; for electrons we shall modify it by a small anisotropy due to the ambient field.

D. REGIONS OF INTERACTION-QUALITATIVE CONSIDERATIONS

The relative importance of the various phenomena which enter into the ionospheric plasma vehicle interaction problem depends on the location of the point in question with respect to the vehicle, the ambient electric field and the velocity vector. Since the general problem is obviously not soluble, even by computation, we must select a series of simpler situations; that is, we must identify a number of "regimes of interaction", in each of which sufficient assumptions are justified to reduce matters to a simple form. From such a set of separate regimes, we may attempt to construct a physical picture of the interaction sufficient for our purposes. We identify the following regimes (Figure 2).

Figure 2
INTERACTION REGIMES



- A. Undisturbed Ionospheric Plasma, with \underline{E}_∞
- B. Disturbed Region $|\underline{r}| \gg \delta_\infty$, Upstream
- B'. Disturbed Region $|\underline{r}| > d_b$, Downstream
- C. Debye Region Upstream
- C'. Debye Region Downstream $\delta_\infty \approx 0$ (d_b).

Region A: This region is far from the body; the plasma is essentially undisturbed but we must take into account the electric field supported by the ionosphere. The electron distribution is slightly anisotropic. As we shall see, a more general, nonuniform electron distribution may be constructed which is applicable nearer the body, and from this an approximate estimate of the surface potential can be made.

Region B: This region is near the body, but outside of the Debye Zone. The local potential and the electron distributions are strongly coupled. Electric neutrality is only approximately preserved; interactions of particles with the surface are of secondary importance. The electron distribution function here is nonuniform with a slight anisotropy due to an external field. This zone is upstream of the body and penetrates to the edge of the Debye region, which is of course very thin here. The ion distribution remains nearly Maxwellian. The reason for this is that the kinetic energy exceeds the thermal energy, at the same time the potential energy of an ion in an electric field arising due to electrical disturbances in the plasma usually is in the order of the thermal energy. Thus the influence of the electric field on the ion distribution function can be neglected.

Region B'-: This is the downstream region for which the same remarks are valid. This region, however, is displaced downstream by a distance of the order of the body dimension, i.e., the zone ahead of it is the downstream Debye region of dimension $O(d_p)$.

Region C: The upstream Debye region. The electric fields in this region are very large (of the order of hundreds of volt/meter). The ion trajectories are not much disturbed by these fields in view of the thinness of the region. The electron distribution, however, is strongly influenced not only by the field but also by surface absorption and reflections so that the distribution function is highly anisotropic and discontinuous.

Region C'-: This is the downstream Debye region. Ions are strongly shaded by the body so that there is a large negative potential in this region which is almost a vacuum. Consequently, electrons are also rejected from this region. The influence on the electric field on ion trajectories cannot be neglected here. This region is certainly the most difficult to treat analytically; the usual assumption which is made is that the region is almost a vacuum and that the effects of space charge are of second order. An approximate solution is therefore derived from the Laplace equation only.

E. THE FAR FIELD: - REGION A

Although collisions have been neglected throughout the remainder of our work they have to be briefly taken into account in the far field. This becomes apparent when we write down the solution to the Vlasov equation for a uniform collisionless plasma, viz,

$$f_e = \exp \left(\frac{e\phi}{kT} \right) f_m(v)$$

where

$$f_m = n_\infty \left(\frac{m_e}{2\pi kT_e} \right)^{3/2} \exp \left\{ - \frac{m_e (v + \underline{V})^2}{2kT_e} \right\}$$

is the Maxwellian and $n_e = n_\infty \exp(\frac{e\phi}{kT})$ is the local electron density. Since $\phi = -E_\infty \underline{k} \cdot \underline{r}$ for a uniform field, we get infinite electron densities as $\underline{r} \rightarrow \infty$. In fact the energy imparted to electrons by the field must be dissipated in collisions and the electron momentum randomized. We have shown that if collisions are taken into account to a first order then an electron distribution function:

$$f_e = n_\infty \left(\frac{m_e}{2\pi kT_e} \right)^{3/2} \exp \left\{ \frac{e}{kT} (\phi + E_\infty \underline{r} \cdot \underline{k}) \right\} \exp \left\{ - \frac{m_e}{2kT_e} (\underline{v} + \underline{V})^2 \right\} \left[1 - \frac{eE_\infty}{kT_e \nu} \underline{k} \cdot \underline{v} \right]$$
 results. Here ν is the (constant) collision frequency. This distribution function can be seen to have the properties:

$$\begin{aligned} f_e &\rightarrow \exp(e\phi/kT) f_m \text{ as } E_\infty \rightarrow 0 \\ f_e &\rightarrow f_m \left[1 - \frac{eE_\infty}{kT_e \nu} \underline{k} \cdot \underline{v} \right] \text{ as } \underline{r} \rightarrow \infty \end{aligned}$$

Thus in the former limit f reduces to the non-uniform Maxwellian, which arises in the work of various authors who have treated this problem without an ambient electric field (8,10). When the influence of the body is removed we obtain a slightly anisotropic distribution function. This is the usual solution for a spatially homogeneous plasma supporting a weak field.

F. THE SURFACE POTENTIAL

The above electron distribution function may be used to make an approximate estimate of the surface potential. We shall consider first a dielectric surface for which the condition:

$$\underline{j}_e \cdot \underline{n} = \bar{R} \underline{j}_i \cdot \underline{n}; \quad \bar{R} = (1 - R_i) / (1 - R_e) \quad (5)$$

must be satisfied locally. Here R_e and R_i are the electron and ion reflection factors (averaged). In keeping with our previous assumption regarding the ion kinetic energy, we may calculate the ion current without reference to the potential field. The electron current, after substitution of Equation (5) is:

$$\begin{aligned} \underline{j}_e \cdot \underline{n} = \exp \left\{ \frac{e(\phi + E_\infty \underline{r} \cdot \underline{k})}{kT} \right\} & \left[\left(1 + \frac{e}{kT\nu} \frac{\partial \phi}{\partial \underline{r}} \cdot \underline{v} \right) \int_{\underline{v} \cdot \underline{n} < 0} f_m \underline{v} \cdot \underline{n} d\underline{v} - \frac{eE_\infty}{kT\nu} \right. \\ & \left. \int_{\underline{v} \cdot \underline{n} < 0} f_m (\underline{v} \cdot \underline{n}) (\underline{v} \cdot \underline{k}) d\underline{v} \right] \end{aligned}$$

The assumption is implicit here that the anisotropy of the far field persists as the plasma penetrates regions closer to the body. We have not attempted to justify this assumption but it can be seen to be reasonable when one considers that the collision

mean free path is large compared with dimensions typical of regions B and C (but not of region A). We may now derive an expression for the surface potential, which becomes after omission of terms of smaller order:

$$\phi_s = -\frac{kT}{e} \ln \left[\frac{1 + \frac{eE_\infty V}{kT v} (\underline{i} \cdot \underline{k} + \frac{v r_s}{V} \underline{p} \cdot \underline{k} + \frac{\sqrt{\pi}}{2 S_\infty} \underline{n} \cdot \underline{k})}{2 \sqrt{\pi} \bar{R} S_\infty (\underline{i} \cdot \underline{n})} \right].$$

When $E_\infty = 0$ this result reduces to the expression given by Alpert, Gurevich, and Pitaevski⁽⁷⁾ for the problem without ambient field. The term in E_∞ contains the angle between the normal to the surface and the electric field and the angle between the electric field and the velocity vector. Here $S_\infty = (m_e V^2 / 2kT)^{1/2}$ is the speed ratio of the undisturbed plasma. The term in $\underline{p} \cdot \underline{k}$ is due to the displacement of the center of coordinates to the surface point in question and is usually negligible. In a typical example for $T = 2000^\circ K$, $V = 8 \times 10^3$ meters/sec., $v = 10^3$ /sec., $|r_s| = 1$ meter, $\underline{i} \cdot \underline{n} = 1$, $\underline{k} \cdot \underline{n} = 1$, $\underline{p} \cdot \underline{k} = 1$; the surface potential was found to be 0.37 volts for $E_\infty = 0$ and 0.51 volts for $E_\infty = 10^{-3}$ volts/meter.

G. THE UPSTREAM NEAR FIELD

The Poisson equation can be written in dimensionless form:

$$\nabla^2 \left(-\frac{e\phi}{kT} \right) = \left(\frac{d}{\delta_\infty} \right) \left[\frac{n_i(\underline{r})}{n_\infty} - \exp \left\{ \frac{E_\infty \underline{r} \cdot \underline{k}}{kT} - \left(-\frac{e\phi}{kT} \right) \right\} \right],$$

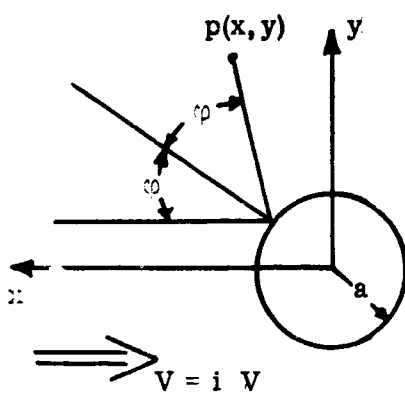
where ∇^2 had been normalized with respect to a typical body dimension d . Since $d \gg \delta_\infty$ it appears that a solution can be sought in the form:

$$\frac{e\phi}{kT} = -\frac{E_\infty \underline{r} \cdot \underline{k}}{kT} + \ln \left(\frac{n_\infty}{n_i(\underline{r})} \right) + O \left(\frac{\delta_\infty^2}{d} \right)$$

Thus the potential is given, to a first order, by the condition of local charge neutrality. This is consistent with our previous qualitative remarks about this regime of interaction. The local electric field is therefore simply the ambient field plus the induced field, the latter being given by the ion density distribution. The effects of surface interactions and of the ambient field on the induced field are of the second order.

This order of approximation is quite adequate for our purposes. The ion density is given by: $n_i(\underline{r}) = n_\infty + n_{i\mu}(\underline{r}) + \delta n_i(\underline{r})$ where $n_{i\mu}(\underline{r})$ is the density of reflected ions and $\delta n_i(\underline{r})$ is the decrement of ion density due to shielding by the body. Clearly, in the upstream regime $\delta n_i(\underline{r}) = 0$ and we are left with the task of calculating $n_{i\mu}(\underline{r})$. Since the electric and magnetic fields can be shown to have only a small influence on the ion trajectories, the problem can be treated kinetically for both specular and diffused reflections. We have given, in our Technical Report, a method for the calculation in the case of specular reflection. Such a calculation can be carried out analytically only for very simple surface shapes; otherwise numerical computing is required. In general, $n_{i\mu}(\underline{r})$ will turn out to be a function of $m_i V^2/2kT$. A considerable simplification can be realized if the thermal motion of ions is neglected altogether; in this case we are dealing with an "infinite Mach number" hypersonic stream of monoenergetic ions.

A simple example of the above procedure is provided by an upstream region of a sphere.



The ion density can be shown to be

$$n_i(\underline{r}) = n_\infty \left[1 + \frac{R_i a^2}{y^2} \frac{\sin^2 \varphi \cos^2 \varphi}{1 - a/y \sin^2 \varphi} \right]$$

where R_i is the ion reflection factor. On the upstream axis of the flow ($y=0$) we find,

$$E = E_\infty + E_{ind} = i \frac{4kTR_i}{ea} \left(2 \frac{x}{a} - 1 \right)^{-1} \left\{ \left(2 \frac{x}{a} - 1 \right)^2 + R_i \right\}^{-1} + E_\infty$$

The function $E_{induced}$ has been plotted in our Technical Report for $R=0.5$ and $T=1000^\circ K$.

It is found that $E_{induced}$ is approximately 0.1 volts/meter just ahead of the Debye region and reduces to less than 0.1 of this value at an upstream distance of one body radius.

H. DOWNSTREAM NEAR FIELD

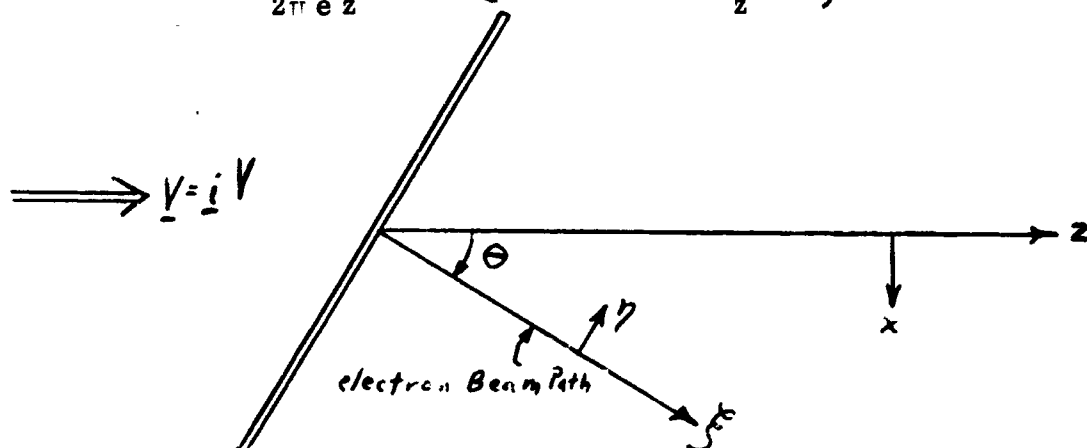
$n_{i\mu}(\underline{r})$, the density of the reflected particles in the shaded zone, is very low so that the task here is to calculate $\delta n_i(\underline{r})$. As an example of the fields

to be expected here we have taken the case of an inclined flat plate of area S . Actually, the downstream ion density will be determined primarily by the cross-sectional shape of the obstacle presented to the free stream. Our results will therefore be valid approximately for other bodies of the same cross-sectional shape. Sufficiently far downstream $\delta n_1(r) \ll n_\infty$ and therefore:

$$\phi = -E_\infty \underline{r} \cdot \underline{k} + \frac{kT}{e} \frac{\delta n_1(r)}{n_\infty} + O\left(\frac{\delta_\infty}{d}\right)^2$$

If x, y, z are the Cartesian coordinates, with z in the downstream direction it can be shown that:

$$\phi = -E_\infty \underline{r} \cdot \underline{k} - \frac{S m_i V^2}{2\pi e z^2} \exp \left\{ -\frac{m_i V^2}{2kT} \frac{x^2 + y^2}{z^2} \right\}$$



If a rectangular plate of area A is placed at angle θ to the stream we find that the induced fields parallel η and perpendicular ξ to the plate are (with $S = A \cos \theta$):

$$-E_{\xi \text{ induced}} = \frac{2kTA}{\pi e \xi^3} \frac{m_i S_\infty^2}{m_e} \sec \theta \exp \left\{ -\frac{m_i S_\infty^2}{m_e} \tan^2 \theta \right\}$$

$$E_{\eta \text{ induced}} = \frac{2kTA}{\pi e \xi^3} \frac{m_i S_\infty^2}{m_e} \sec \theta \tan \theta \left(\frac{m_i S_\infty^2}{m_e} \sec^2 \theta - 1 \right) \exp \left\{ -\frac{m_i S_\infty^2}{m_e} \tan^2 \theta \right\}$$

These results have been illustrated in our Technical Report. The plate A may be regarded as an electron beam collector plate. The field E_{induced} would then be

transverse to the beam and give rise to a deflection. Our results show that this field is zero for $\Theta = 0$ and increases with Θ to a maximum value of about $0.14/\xi$ v/meter, where ξ is in meters. If Θ is increased beyond this value the field decreases again as the point at which it is being evaluated moves out of the wake of the plate.

I. UPSTREAM DEBYE REGION

In this region the particle density is high (but certainly not more than twice the ambient density) so that the thickness of the region must be of the order of the Debye length based on ambient electron density. The electron distribution function here is highly dependent on surface effects and is anisotropic and discontinuous. If the surface is a conductor the electric field is certainly normal there and can be shown to be nearly normal throughout the region. Gradients of all variables in the tangential direction must be small, so that the problem can be reduced to the solution of the one dimensional Vlasov and Poisson equations:

$$u \frac{\partial f}{\partial x} + \frac{e}{m} \frac{\partial \phi}{\partial x} \frac{\partial f}{\partial u} = 0; \quad \frac{d^2 \phi}{dx^2} = 4\pi e \left\{ \int f_e d\mathbf{v} - n_1(x) \right\}$$

The solution to the former is: $f = f(v, w, \epsilon)$ and $\epsilon = 1/2 m_e u^2 - e \phi$

where u, x , are normal to the surface and y, z, v , and w , are tangential. (The solution to the Vlasov equation is a function of the constants of the motion of an electron in the potential).

For this regime we have put forward an extension of a method due to Pung and Ziering.⁽⁹⁾ Their approach is to consider separately incoming and receding particles and to write separate distribution functions for particles with sufficient or insufficient energy to reach the surface, for receding particles which have suffered specular or diffused reflection and for emitted particles. We have extended the problem to take account of an anisotropy in the distribution at the edge of the sheath and derived expressions for the electron density in the sheath for the case of complete absorption at the surface. Our results, however, contain integrals which cannot be expressed in terms of tabulated functions. Our treatment is therefore incomplete.

J. THE DOWNSTREAM DEBYE REGION

This region is of the order of a body dimension in extent and conditions here are highly non-uniform. The problem is much too difficult to treat in its general form. It can be shown, however, that the ion density (in view of strong shading by the body) is of order $(\delta/d)^2 n_\infty$. The potential can be written:

$$\frac{e\phi}{kT} = \frac{e\phi^{(0)}}{kT} + \left(\frac{d}{\delta_\infty}\right)^2 \frac{e\phi^{(1)}}{kT} + O\left(\left(\frac{d}{\delta_\infty}\right)^2\right)$$

When this is substituted into the Poisson equation it can be shown that the Laplacian is of higher order than the term containing n_i and n_e . That is, the contribution of space charge is of the second order. An approximation to the potential distribution can be obtained by dealing only with the Laplace equation, the boundary condition $\phi = \bar{\phi}_s$ at the surface, and the condition on ξ junction of region B'. This procedure is the reverse of that adopted for the near field, where we calculated the potential from the condition of charge neutrality and regarded the contribution of the Laplace as a perturbation.

The methods of dealing with the Laplace equation are well known, but we have given only a simple two dimensional example, since the body shape is not yet specified. It can be shown, however, that the electric fields in this region are of order:

$$\frac{1}{10d} \ln \left(\frac{2\delta_\infty}{d} \right)$$

in the direction of the free stream and approximately an order of magnitude higher in the transverse direction. Under the conditions of interest to us, the latter field would be of the order of 40 volts/meter for a 5 cm collector plate. It is important therefore that the beam be oriented so that as little as possible of its path lies in the wake of either the gun housing or the collector plate.

K. CONCLUSIONS

We have investigated various regions of interaction between the ionospheric plasma and surfaces moving at satellite velocities. In its most general form the problem involves the simultaneous solution of the Boltzmann and Poisson equations plus surface conditions for the impingement of particles. To derive rapid methods of estimation for the induced electric fields we have divided the problem into:

- 1) The Far Field,
 - 2) The Near Field, without surface conditions,
- and
- 3) The Debye Regions, upstream and downstream of the body.

Since no specific shape or property of surface is given our work has been of an illustrative nature; the principle result being that we have assembled the methods which can be used for suitable calculations when the problem is more completely specified. However, the order of magnitude of the induced electric fields has been estimated for the various regimes of interaction, so that some reasonably adequate guidelines for the operation of the electron beam field meter and the interpretation of the data can be given.

The following are our principle conclusions:

- 1) We have given an electron distribution function valid in the far field and the near field. The effect of an ambient electric field due to ionospheric phenomena is to produce a small anisotropy in this distribution function.
- 2) The effect of induced and ambient electric fields on the motion of ions can be neglected. With the exception of certain circumstances in which a magnetic field can facilitate the penetration of ions into the shaded region behind the obstacle, the effect of the geomagnetic field on the motion of ions can also be neglected (as far as our present interaction problem is concerned).

- 3) We have given a simple expression for the local potential of a dielectric surface and indicated how the potential for a conducting surface is to be calculated when the shape of the surface has been specified. Our expression is a function of the orientation of the velocity vector, surface normal vector, and ambient electric field vector.
- 4) The potential in the near field can be calculated, to a first order, from the condition of local charge neutrality. The problem therefore reduces to that of the kinematics and reflection of ions. We have put forward a method for the calculation of the density of ions reflected from the upstream surface.
- 5) Two illustrations of the potential distribution in the near field region have been given. The first applies to the regime upstream of a sphere. We have shown that the induced field on the axis is of the order of $0.1 a^{-1}$ volts/meter (where a meters is the radius of the sphere) near the stagnation point (but outside the Debye region) and decays to approximately 10% of this value one body radius upstream of the stagnation point. The parameters in this example are typical of those expected in the E and F regions of the ionosphere. The details of such a calculation become more complicated for other blunt shapes, but the order of magnitude of the induced fields are expected to be about the same.
- 6) Our second example for the near field concerns the region downstream of an obstacle of arbitrary cross-sectional shape; a numerical example is given for an inclined flat plate typical of the electron beam gun housing or collector plate. This region is more than one body dimension downstream of the rear surface; upstream of it lies the Debye region which is here of the order of one body dimension in extent. In our example we have given expressions for the induced electric fields in the directions parallel and perpendicular to the electron beam path.
- 7) As regards the upstream Debye region, which is less than $\alpha 1$ cm in depth, we have shown that the electric field in this regime remains perpendicular to the surface accurate to quantities of the second order.

The problem of the upstream sheath can therefore be treated on a one dimensional basis. We have adapted a method due to previous authors to the case where the electron distribution function is anisotropic at the edge of the sheath. However, certain integrals arise which would have to be computed numerically and this has not been done.

- 8) Since ions are strongly shaded by the body, the downstream Debye region presents an extremely difficult problem, which we have not attempted. It can be shown however that the solution to the Laplace equation is a good approximation to the potential in this region. The effect of space charge is of the second order. The boundary conditions are mixed, since we know the potential of the surface and the electric field at the junction of this Debye region and the downstream "near field". Here again, no specific problem has been posed and we have contented ourselves with an example of a region bounded by an inclined two dimensional flat plate and a uniform electric field at infinity.
- 9) As far as the operation of the electron beam field meter is concerned (assuming that this is placed sufficiently far from the influence of the carrier vehicle) we conclude that the effect of fields induced by the components of the instrument would be most severe when the beam path is nearly parallel to the direction of motion. In this case a large fraction of the beam path would lie in the wake of either the gun housing or collector plate, in which region transverse electric fields of the order of 10 to 100 volts/meter are to be expected. If the beam trajectory is of the order of 10 times the component dimension the angle between beam path and velocity vector should be no less than 20° . The effect of residual fields in the Debye region and the near wake can then be estimated when the geometry is specified.

SECTION III

INSTRUMENT DESIGN AND PERFORMANCE

A. CONCEPTS

There are two major difficulties in measuring ionospheric electric fields by deflection of an electron beam. The first is that the deflection is very small. The second is that the earth magnetic field introduces a very large deflection. Figure 3 illustrates the sensitivities of the beam to both magnetic and electric fields. Note that for a 300 volt beam a magnetic field of 1 gamma produces as much deflection as an electric field of 11 millivolts/meter. Since the earth's field can be of the order of 40,000 gamma, a signal to noise ratio of 1/440,000 must be overcome in order to resolve one millivolt/meter.

Although it is conceivable that the magnetic field could be measured and the correction applied by subtraction, it is apparent from the foregoing that such an approach is not practical.

The means chosen to discriminate between the deflection due to magnetic versus electric fields is to modulate the electric field in a precise manner, by alternately creating and removing a Faraday shield around the beam. The magnetic field is unaffected by this, while the electric field is modulated in a square-wave fashion. By demodulating the output signal synchronously with the modulation, only the square-wave signal is accepted. In order to accurately measure deflections without requiring an extremely accurate mosaic target or other such device, the closed loop beam centering system is employed. A current collector target is divided into four segments as shown in Figure 4. The currents collected in two opposing segments are balanced against each other. The difference signal is amplified and applied as the voltage to an appropriate pair of deflection plates to keep the spot centered on the target. The voltage on the deflection plates is then a direct measure of the field induced beam deflection. The component of this voltage which is synchronous with the chopper represents the electric field while the steady state voltage represents the magnetic field. It should also be noted that there is virtually no requirement on drift or d.c.

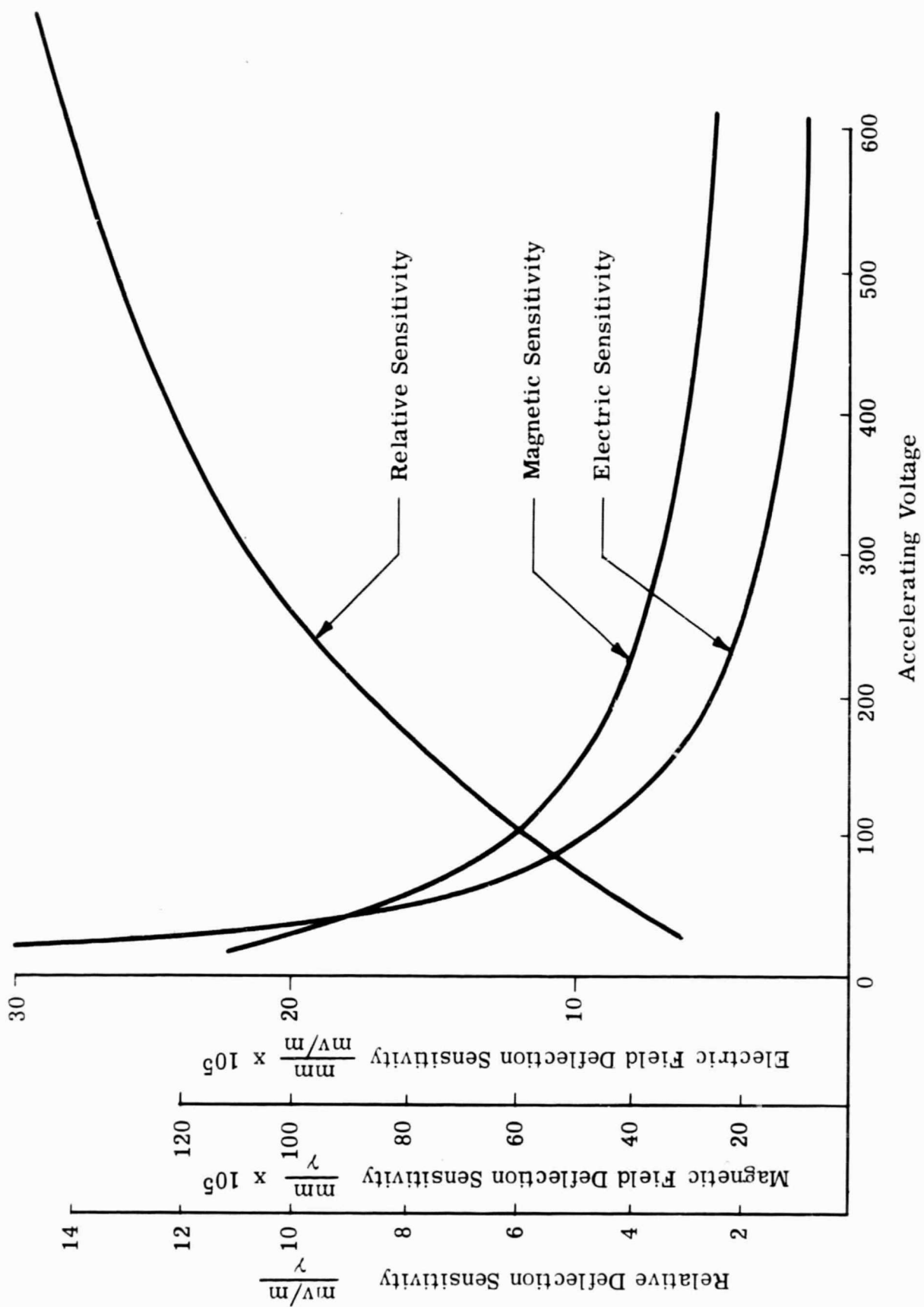


Figure 3 : Beam Sensitivities

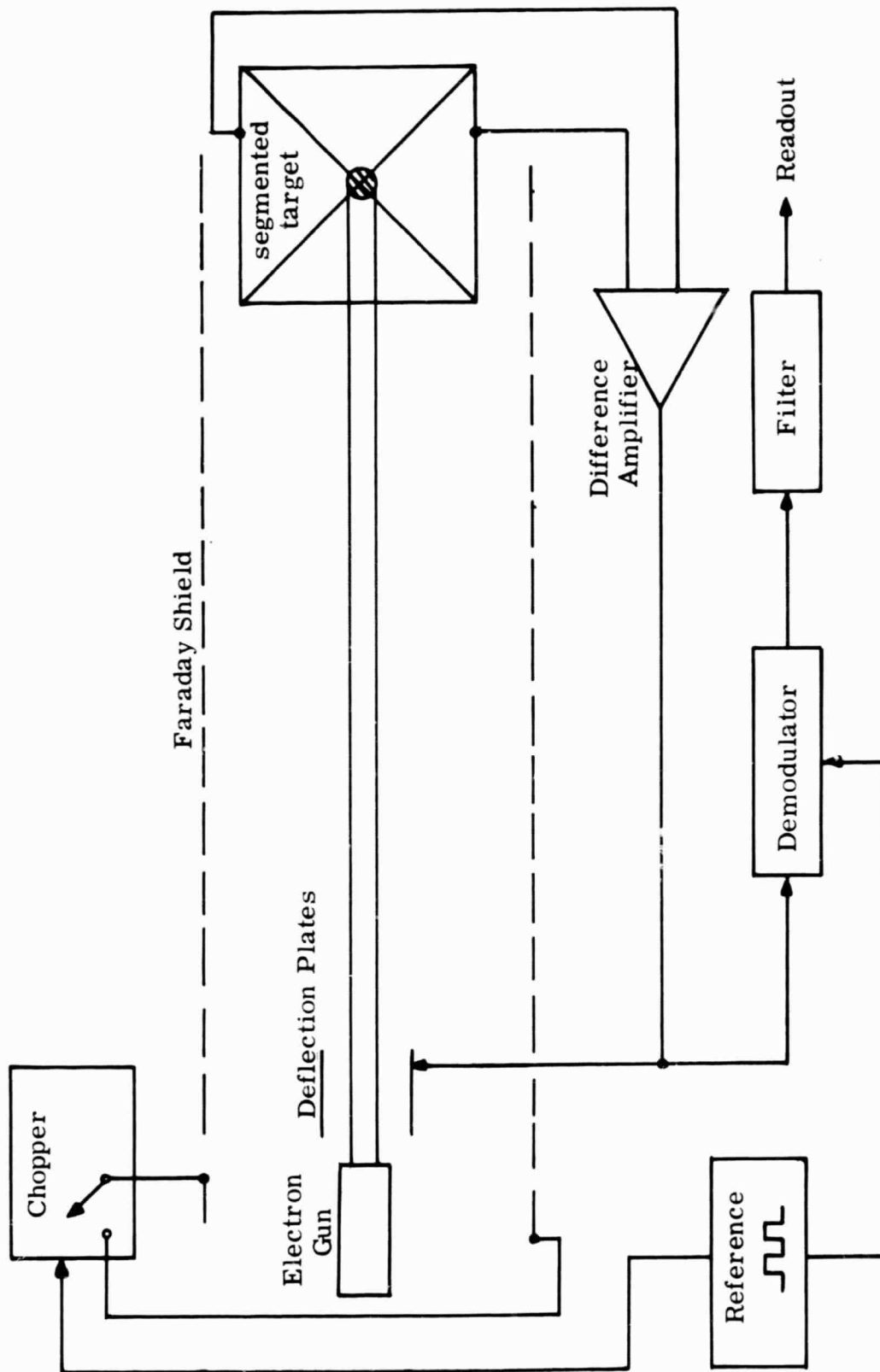


Figure 4 : Electrostatic Field Meter (Single Axis Shown)

offset of the amplifiers in the loop, or on mechanical or thermal stability. Any misalignments in the gun-target arrangement will contribute to the d.c. deflection plate voltage and will not affect the electric field reading.

B. COMPONENT DESCRIPTION

Figure 5 is a functional block diagram of the meter showing some of the parameters of the loop. The conversion constants from electric and magnetic field to deflection are based on a 500 volt beam. A realistic design goal for the accuracy of this meter would be $\pm 1 \text{ mv/m}$ over a range of 10 mv/m to 100 mv/m and 1 or 2% accuracy over a dynamic range of 100 mv/m to 1000 volts/meter . The upper limit is determined by the $\pm 100 \text{ volts}$ limitation of the readout equipment and power supplies. The equipment as breadboarded to date is shown in Figure 6. A somewhat more detailed description of each component follows.

1. Electron Gun and Beam

The electron gun design chosen for the electric field meter is the electrostatic lens, hairpin filament type. This design provides a rugged, reliable gun which can provide an electron beam having a diameter of 1 mm or less, and focussed at distances up to 25 cm for accelerating voltages between 300 - 500 volts.

The electron gun being used in the laboratory experimental unit is the Superior Electronic Corporation, Type SE-2B, modified with a tungsten replaceable filament.

The beam current at the target is 1 microampere at a pressure of 10^{-5} torr. The filament is operated space charge limited drawing 3.6 amperes at 3 volts.

The control grid is biased positive at 21 volts and the focus electrode is operated at 120 volts. The cathode is negative 500 volts with respect to the grounded final accelerating anode. The filament is the cathode, and the acceleration potential is applied in a balanced method across the hairpin filament. Both a.c. and d.c. filament power has been used. Figure 7 illustrates the gun hookup.

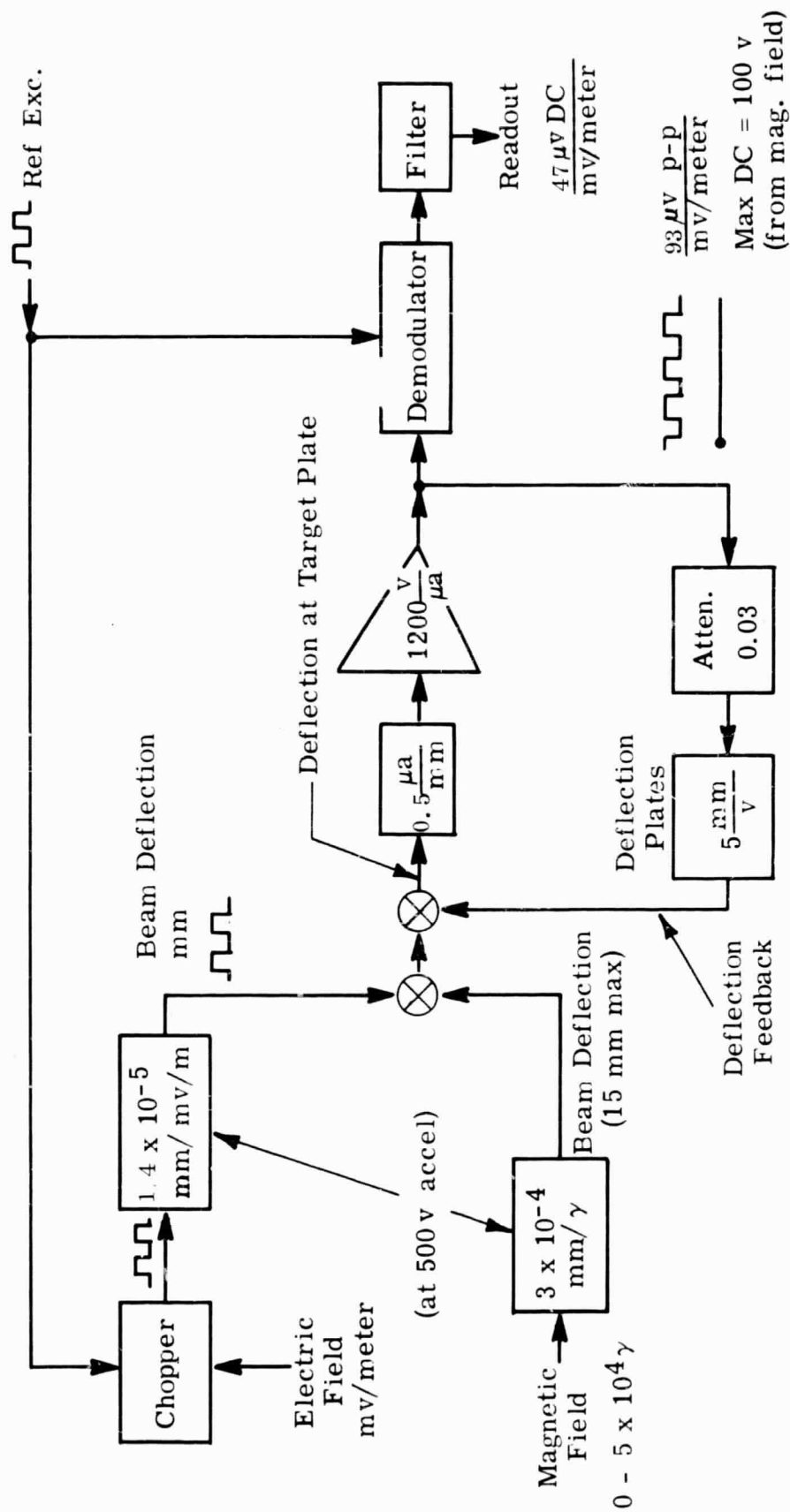


Figure 5 : Electric Field Meter System - Block Diagram (Single Axis Shown)

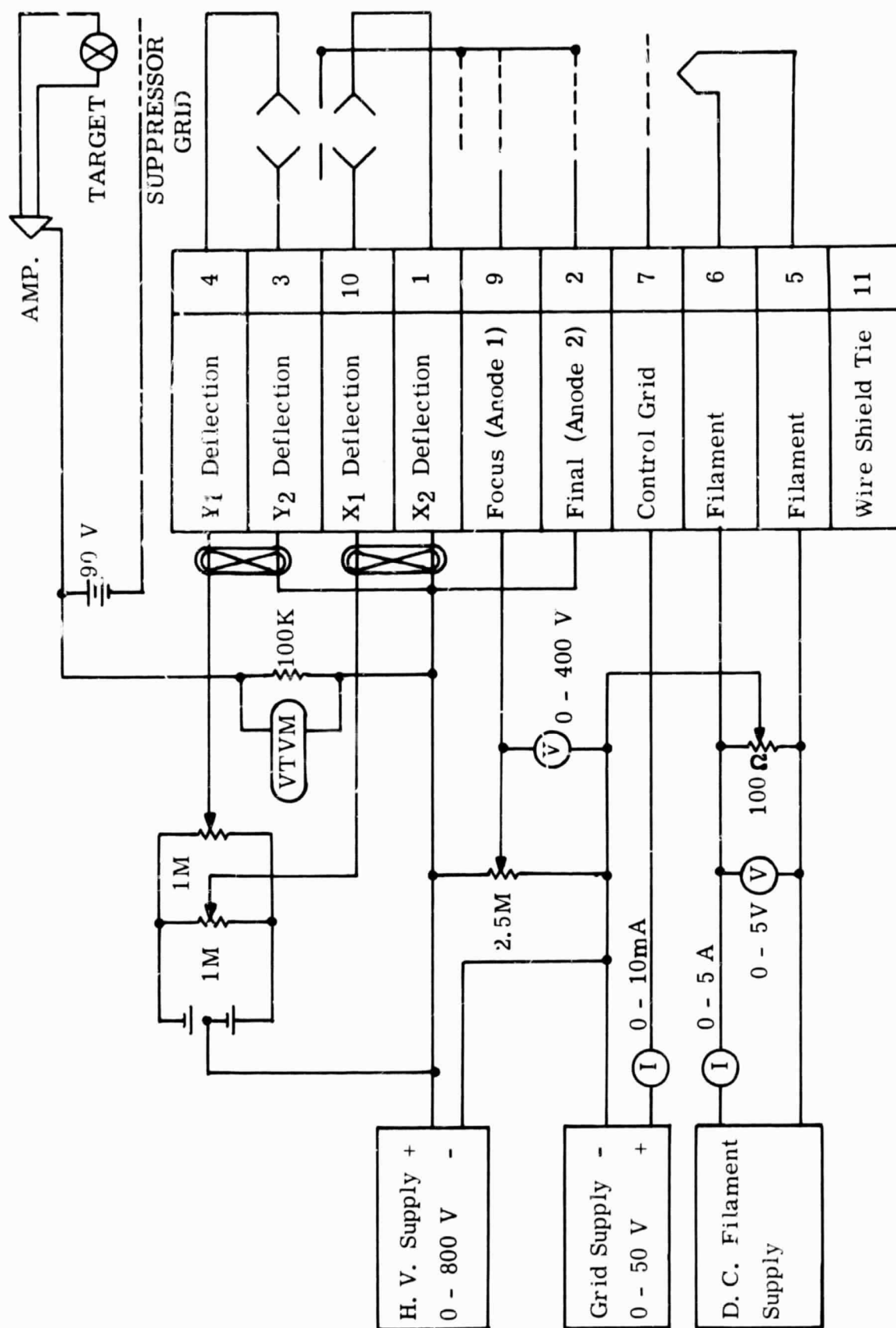


Figure 7 : Gun Voltages

2. Target

The target presently used is made by depositing pure gold onto a flat glass surface. Leads are attached by means of silver filled conducting epoxy and lamp black is then deposited over the gold by holding the plate in a candle flame. The target is segmented into four isolated sections by scribing with a sharp stylus. A light dusting of optically active ZnS is applied all over the target except for a 1/4-inch diameter circle centered on the target center. This is for convenience in finding and focussing the beam. The purpose of the carbon is to protect the gold from the beam energy, as well as to give a somewhat lower secondary electron emission. One of the major problems was found to be secondary emission. A suppressor grid located 1/4-inch in front of the target plate and kept at a negative 90 volt potential with respect to the target was found to suppress secondary electrons sufficiently to allow the loop to operate. An open loop measurement on the breadboard showed that using the suppressor grid the target's conversion scale factor is .3 to .5 microamps per mm deflection.

3. Deflection Centering Loop

a. Differential Current Amplifier

The first section consists of a current comparator circuit using an operational amplifier (A_1 in Figure 6). This circuit converts a current unbalanced signal to a voltage with low source impedance. The scale factor for this conversion is equal to the value of the feedback and input resistance, 1.1 megohms, in this case. The amplifier and resistor are located directly behind the target plate to minimize pickup problems.

b. Voltage Gain Section

Operational amplifiers A_2 and A_3 provide a voltage gain of 1200 with a maximum linear output of ± 100 volts. The phase shift characteristic is shaped to permit stable closed loop operation.

c. Feedback Attenuator and Output Scale Factor

The scale factor of the output is proportional to the reciprocal of the attenuation in the feedback loop. The maximum scale factor is selected on the

basis of the maximum d.c. output available to balance the maximum deflection due to magnetic fields. With a ± 100 volt limit on the d.c. output, the scale factor is $30 \frac{\mu v}{mv/m}$.

d. Deflection Plates

The sensitivity of the deflection plates is approximately 2.4 mm/v for each plate. When both plates are driven in push-pull fashion the gain is 5 mm/v.

4. Faraday Cage

Modulation of an electric field in an ionized medium as conceived for the field meter has not yet been demonstrated in the laboratory. It is quite difficult to simulate the properties of the ionosphere and indeed it is questionable whether an adequate simulation is even feasible. For the breadboard tests to date a Faraday screen was constructed, consisting of a pair of 1/2-inch mesh screens on each axis. A voltage applied as a square wave across one axis produces a chopped field perpendicular to the beam.

5. Detector and Filter

The deflection plate voltage is coupled through a high pass filter to the chopper. The purpose of this is to suppress much of the flicker noise from the amplifiers. The demodulator is a capacitor coupled type with SPST switch. The chopper presently used is a standard Airpax series 600 which contains two synchronized poles in one package. The other pole is used for field modulation. The filter section consists of two RC sections. The high frequency response of the instrument is determined by this filter. In this case the cut off is set at 1/2 cps primarily because of the high level of back-ground line frequency interference which must be filtered out at this point.

6. Readout

The readout used in the laboratory testing is a John H. Fluke differential a.c. - d.c. voltmeter, which is capable of resolving 0.1 mv d.c.

C. ENVIRONMENT

1. Vacuum System

The electric field meter is placed within an 18 inch diameter bell jar, which is 30 inches in height. The vacuum system is a 4 inch oil diffusion pump, Vactronic HVS4000 which is sustained through a mechanical pump, Welch 1397. A liquid nitrogen cold trap is in the line to the bell jar. Vacuum as low as 10^{-6} torr is maintained in the bell jar without the electron gun heated, and normal operation is a 5×10^{-6} torr with all systems of the meter operative. The pressure is measured by an ionized pressure gauge C.E.C. Model GIC-110, within the bell jar.

The experimental support structure was carefully designed to allow trapped gas to escape from screw threads and low outgassing material was used.

2. Spurious Field Interference

No attempt was made to isolate the meter from background power line interference. As a result the beam is subject to a.c. magnetic fields far in excess of anything that can be expected in a space application. The filter used in the laboratory has been selected to reduce this component of the output sufficiently so that the d.c. signal of interest can be readout. For a mission-designed instrument of course this filter will be redesigned. A side benefit of the pickup is that when it appears at the amplifier output (before demodulation and filtering) it gives a good visual indication that the beam is centered and focussed. Initial beam centering and fine focussing is greatly facilitated by this and it may be desirable in the future to provide a known a.c. field specifically for this purpose in calibration setups.

3. Mechanical Vibration and Isolation

It has not been found necessary to take any precautions against mechanical vibration beyond the initial step of isolating the roughing pump from the chamber. This was done by using a soft rubber tube which was solidly clamped to ground near its center.

D. LABORATORY TEST PROCEDURE

To operate the field meter the following steps are followed:

- 1) Check vacuum: Pressure should be less than 10^{-5} torr.
- 2) Bring filament voltage slowly up until filament current is 3 amperes. Wait for pressure to rise and fall again. Bring filament current to 3.6 amperes.
- 3) Turn on gun voltages, amplifier power, and bias supplies.
- 4) If beam has been previously centered and adjustments have not been disturbed the beam is now operative. If initial adjustments are being made the following steps are followed:

- a) Disconnect deflection plates from amplifier output (both axes). Ground deflection plates. Set initial voltages

Acceleration voltage = 500 v

Focus voltage = 120 v

Control grid voltage = + 21 v

Suppressor grid voltage = - 90 v

- b) Sweep X and Y deflection voltages systematically until spot is located.
- c) Bring spot to a place on target where it can be seen clearly.
- d) Trim focus and grid voltages to give well focussed spot, approximately 1 mm in diameter.
- e) Bring spot to center of target.

- f) Observe output of A_3 for both X and Y axes. Adjust X and Y focussing, control grid, and centering controls to get maximum output from each axis without saturation. Close loop by re-connecting deflection plates to A_3 outputs. The loop is now operating, and the field may be applied.

E. LABORATORY PERFORMANCE

1. Setup

Figure 8 shows the setup used for measuring the input-output characteristics of the meter.

2. Loop Output Characteristic

The attenuator was arbitrarily adjusted to give a somewhat greater sensitivity than that shown in Figure 5. This was at the expense of d.c. range, but in the fixed environment of the laboratory all the d.c. offsets were taken into account by adjustment of the centering controls. Datapoints were taken from 5mv/meter to 4v/meter. Periodically a zero check was made and a zero correction was applied to all readings. The zero offset is unexplained, but since the readings are repeatable, it is felt that this offset, if not reduced to negligible proportion, can be taken into account by zero field calibration in flight. The data points for the X and Y axis are shown in Figures 9 and 10. The Y axis showed a scale factor of $83 \frac{\mu V}{mv/meter}$. Two runs were made and the worst deviation was 3mv/meter at 40 mv/meter. The X axis showed a slope of $66 \frac{\mu V}{mv/meter}$ with similar repeatability.

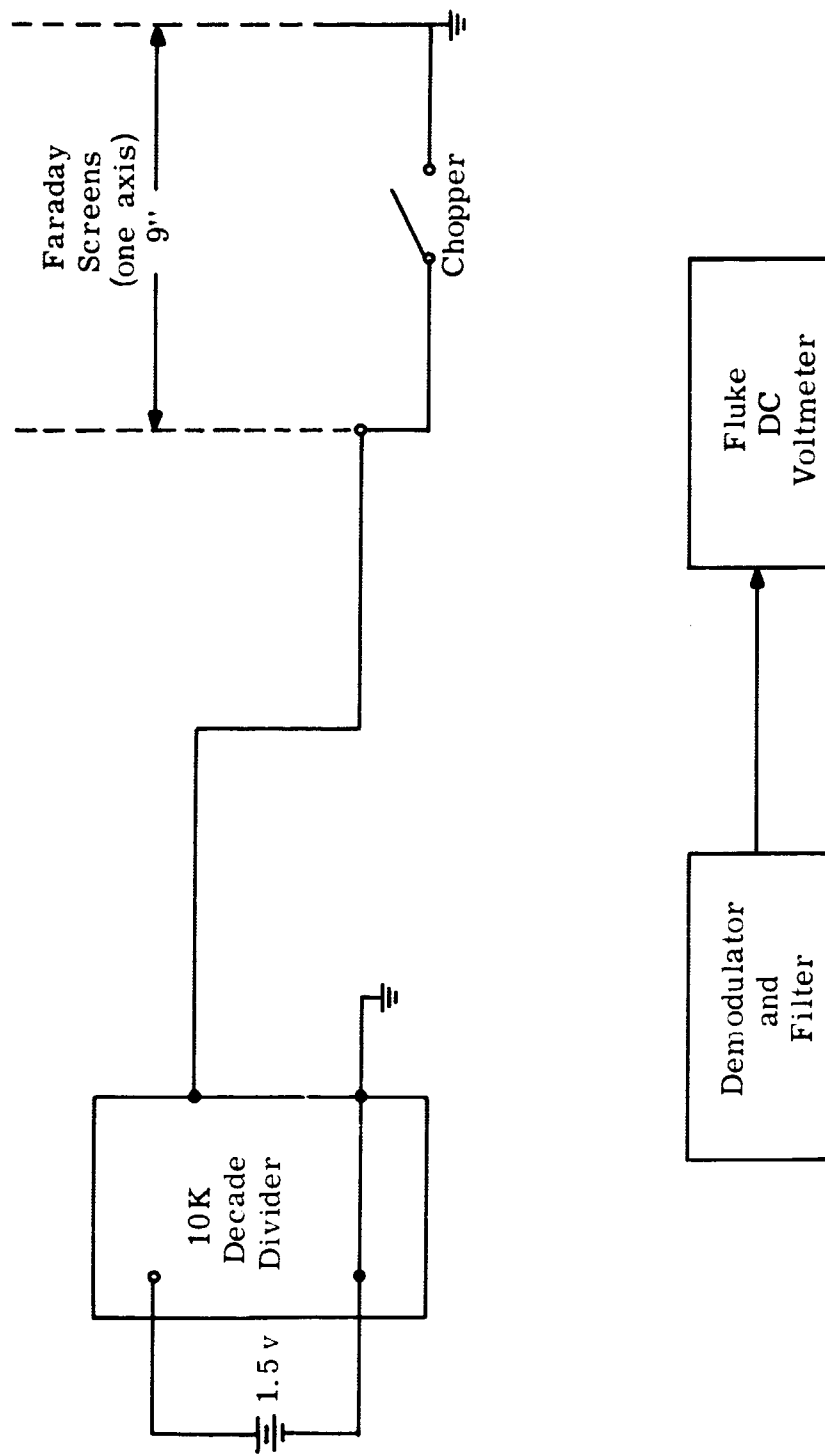


Figure 8 : Scale Factor Measurement

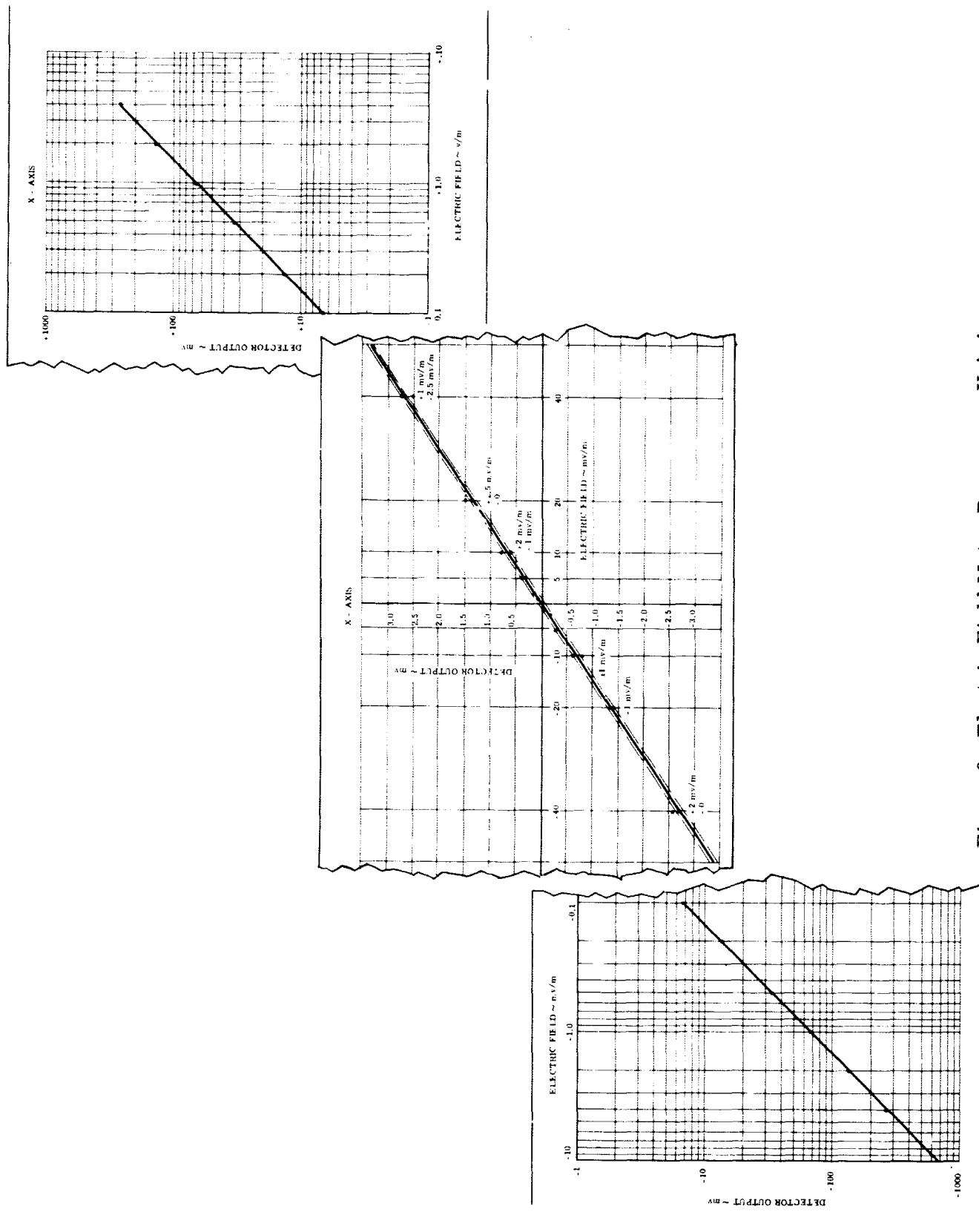


Figure 9: Electric Field Meter Response - X Axis

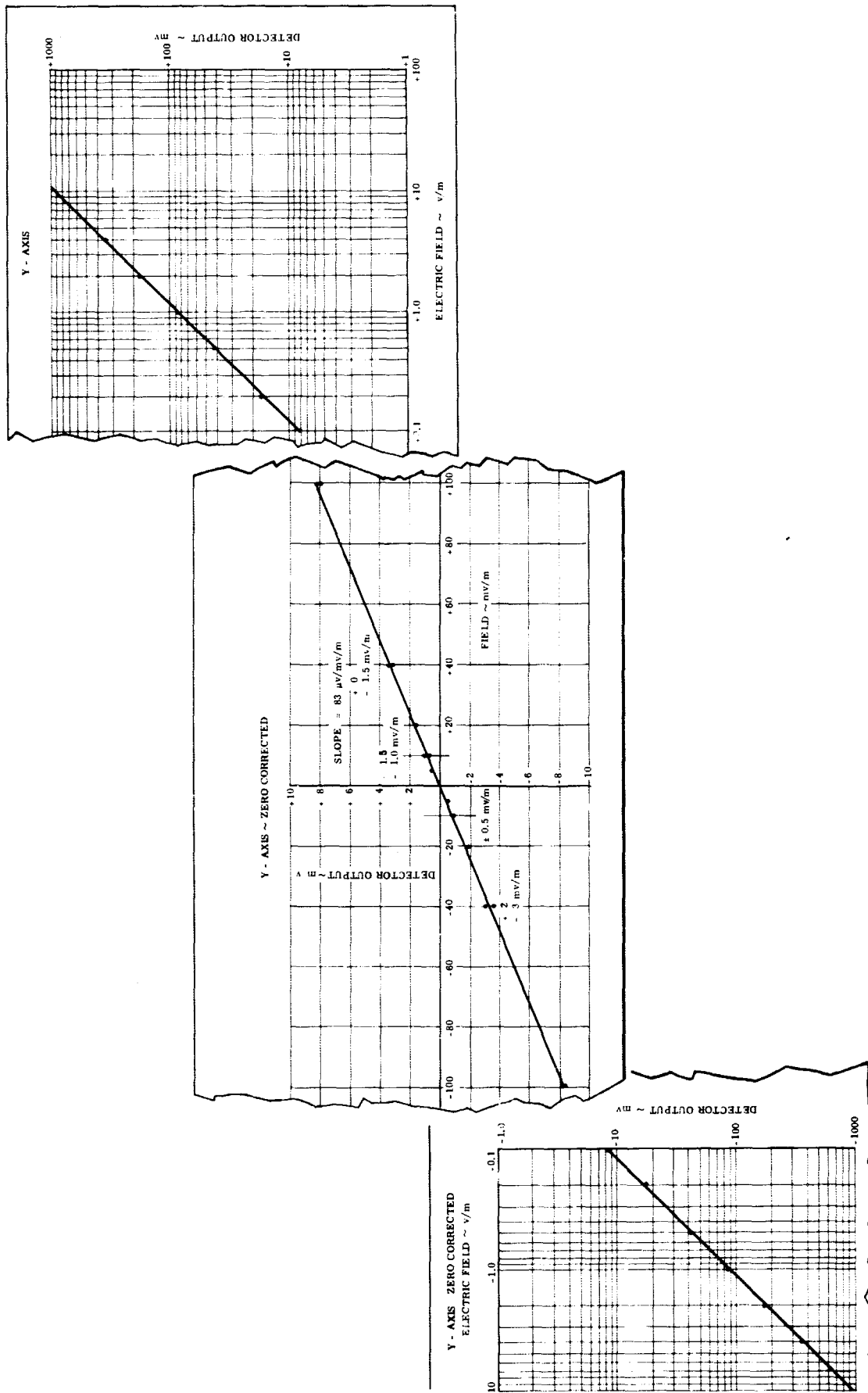


Figure 10: Electric Field Meter Response - Y Axis

PRECEDING PAGE BLANK NOT FILMED.

SECTION IV

MISSION CONSIDERATIONS

A. MISSION CATEGORIES

The potential missions for which an electron beam deflection electric field meter would provide the required information can be divided in two categories:

- 1) Engineering or Housekeeping
- 2) Scientific or Survey

These measurement missions were briefly mentioned in the introduction of this report and are divided as follows:

1. Category I - Engineering or Housekeeping:

- a) Electric fields associated with charge particulate contaminant clouds caused by the efflux of materials from a spacecraft. These clouds present a potential hazard to optical and electromagnetic experiments and observations required in performing the mission of the flight. (12)
- b) Electric fields which are associated with the plasma sheath which surrounds the spacecraft. These electric fields are associated with the charge separation which occurs within the sheath, and correlate with experiments modifying the sheath as well as the sheath's influence upon experiments. (13, 14, 15)
- c) Large charged bodies moving within the magnetosphere experience reaction force. Part of this force is caused by the charged body moving through the ambient electric fields that exist within the ionosphere. This force can produce drag and moments on the charged bodies. (16-28)
- d) In the lunar space environment, the ambient electron density and particle density are extremely low. Thus, during the rendezvous and docking of the Lunar Excursion Module with

the orbiting spacecraft, electric fields may exist. The electric field survey of the space between these vehicles would provide confidence that no hazardous situation exists. (29)

2. Category II - Scientific or Survey:

- a) There is evidence both theoretical and measured that electric fields exist within the ionosphere. The variation of these fields are attributed to, or are the cause of, various phenomena observed within the ionosphere and magnetosphere. A survey of this field as extensive as the surveys of the magnetic field will provide the required information to better understand the earth's environment. Surveys taken on long duration missions covering different altitudes, light conditions, seasons, and solar wind conditions will provide the basis for improved models of magnetosphere - solar wind interactions, auroral display, red arc occurrences, and equatorial jet phenomena. Space weather predictions will also be aided, as well as providing another means of observing nuclear explosions in space.
- b) Specific sounding rocket measurements within or above auroral displays will provide correlation of the electric field measurements performed by various electrostatic potential probes and barium vapor cloud experiments.

B. MISSION CONCEPTS

The intrinsic values of the electron beam electric field meter are:

- Wide dynamic range (five orders of magnitude),
- Sensitive to weak fields (10 millivolts/meter field measured with a sensitivity of ± 1 millivolt/meter),
- Non-interaction sensing element (less than 1 micro-ampere electron beam).

These attributes permit the meter to be versatile, capable of performing the various missions previously mentioned.

With the exception of the sounding rocket experiments, all other missions could be performed sequentially on a multipurpose spacecraft such as the AAP workshop. The use of extensible boom and multiple meters will permit the performance of the various experiments by the placement of the meters at the appropriate positions to measure the associated electric fields.

1. Category I - Engineering or Housekeeping Missions:

- a. Charged Contaminant Cloud Electric Fields

One of the most serious problems that faces optical missions is the generation of particulate clouds. The probability that these obscuring clouds are charged due to photoemission or the efflux process is reasonably strong. Thus the measurement of electric fields between the spacecraft and the clouds in the vicinity of optical ports provide an indication of the formation of these charged clouds. The correlation of the electric field measurements and the consequences of various avoidance and removal techniques that will be developed to alleviate the contaminant problem provide a means to develop and evaluate these techniques.

The electric field that will prevail between the spacecraft and the cloud is dependent upon the relative difference of their charges, their respective geometries, the distance between them and the conductivity of the media between them. An estimate of the range of electric field from 10 millivolts/meter to 100 volts/meter includes a wide variety of combinations of these parameters. The possible distance over which the fields exist from just outside the plasma sheath to within 5 body radii from the spacecraft provides a measuring range that includes most of the possible cloud-spacecraft geometries. Beyond this range, the cloud should diffuse sufficiently so as not to represent an optical problem.

- b. Sheath Interaction Electric Fields

The analysis presented in Section II of this report discusses the electric fields associated with the plasma sheath surrounding the spacecraft. Fields across this sheath vary from 1 volt/meter to 1000 volt/meter depending upon the altitude of the vehicle within the ionosphere, the degree of photoemission, and the position of the station at which the field measurement is being made

relative to the velocity direction. The measurement of unperturbed sheath fields is necessary to provide a basis to determine the additional fields due to charge contaminant cloud formation.

In addition the plasma sheath is disturbed by the efflux of charged particles from the surface and the performance of electromagnetic experiments aboard the spacecraft. Finally, the plasma sheath can interfere with experiments being conducted aboard.

The measurement of the electric fields on the surface and in the near vicinity of the spacecraft provides data of the environmental field and its variation. Correlation of these variations with the data obtained by the other experiments aboard provides a better understanding of the phenomena they are observing.

c. Forces and Moments Due to Ionospheric Electric Fields

The observed decay rates of vehicles orbiting with the ionosphere do not correlate well with density measurements. Residuals in the mean motion have been equated to unknown variations in the atmospheric density via the relatively well-quantified aerodynamic forces. A charged body moving through an ambient electric field experiences an electrodynamic force. This force can contribute to orbit decay and, when taken into account as a perturbative influence, can lead to a reassessment of the inferred spatial and temporal variations in ionospheric density. For example at an altitude of 1300 km the aerodynamic force on a 1 meter radius sphere is about 10^{-9} newtons, while the electrodynamic force is of the same order of intensity.

Thus a mission designed to measure the electrodynamic force will provide the first complete set of data from which electrodynamic drag may be directly inferred. Future space programs will benefit by providing a more complete specification of the force and moment environment.

The electrodynamic force requires the measurement of the ambient electric field (E_{∞}) and the surface electric field (E_s). When the distortion from

spherical symmetry of the plasma sheath is considered, the reaction force experience by a spherical body is:

$$\vec{F} = - 2 \pi \epsilon r^2 (\vec{E}_S \cdot \hat{n}) \vec{E}_\infty \text{ Newtons}$$

where:

- r is the body radius in meters
- E_S is the surface electric field in volts/meter
- n is the outward directed surface normal
- E_∞ is the ambient ionospheric electric field in volts/meter
- ϵ is the electric permittivity of the media 'n farads/meter

The performance of this mission requires a surface electric field meter and an ambient electric field meter. The ambient electric field approximately exists beyond a distance of 5 body radii from the spacecraft. The decay of the spacecraft electric field depends upon the ionospheric parameters and the geometry of the spacecraft. In section II of the report the decay of the electric field is discussed. This choice of 5 body radii from mission flown between 200 km and 2000 km altitude, assures degradation of spacecraft fields sufficiently below ambient field levels

The range of electric field values are:

Surface Electric Field:	from 1 volt/meter up to 1000 volts/meter
Ambient Ionospheric Electric Fields:	from 10^{-2} volts/meter up to 1 volt/meter

The precision with which the electrodynamic force is determined depends upon the number of surface field measuring stations that are used. Each measurement results in a local reaction force; if sufficient measurements are made around the spacecraft, the integrated force acting upon the spacecraft can then be determined.

d. **Electric Fields During Rendezvous in a Lunar Environment**

The differential charge build-up of an excursion module on the lunar surface for periods up to two weeks in the sun, as compared to the orbiting spacecraft which is alternately in the dark and light present a potential hazard during rendezvous. Since the environment is of extremely low density, charges do not redistribute rapidly. Thus excessive charge located on the excursion module may exist during rendezvous. An electric field monitor examining the space between the two vehicles can warn of a potentially dangerous field which exists. Shorting rods can then be applied to neutralize the charge difference permitting the docking maneuver to proceed. The wide dynamic range of the meter permits the observation of the build-up of the electric field over large distances, thus allowing sufficient time to take corrective action.

2. **Category II - Scientific or Survey Missions:**

a. **Ambient Electric Field Survey Within the Ionosphere**

The electric field ambient within the ionosphere has been measured to vary from less than 10 millivolts/meter to slightly greater than 100 millivolts meter. The electric field is maximum perpendicular to the magnetic field lines due to the tensor conductivity of the ionosphere, and is generally directed toward the equator.

The weak electric fields, the ionization of the environment, and the apparent electric field due to the motion of the instrument through the magnetosphere have made measurements of these fields extremely difficult.

The design of the electron beam electric field meter considered the sensitivity and plasma wake requirements as previously discussed, while the apparent electric field is considered in the following sections with regard to the demands placed upon the spacecraft attitude resolution requirements.

b. **Sounding Rocket Exploration of Auroral Electric Fields**

Many experimenters have flown near vertical sounding rocket flight in the auroral display regime with a variety of electric field measurement devices.

The choice of the vertical flight is the near cancellation of the apparent ($\vec{v} \times \vec{B}$) field due to the motion through the magnetosphere. There is general correlation of the range of intensity and direction of the electric field during an auroral display.

The electron beam field meter would provide measurements which could be compared with those of many instruments and techniques that have been used to examine the electric fields.

C. METER CONSTRAINTS

The use of the electron beam electric field meter within the ionosphere is restricted by various environmental considerations. These constraints include the following:

- Orientation of the meter to the flow field
- Location of electron beam relative to physical structures
- Meter measures two orthogonal field components
- Outgassing, secondary emission and photoemission influence on the electron beam parameters
- EM I and RF I caused by the device or within the environment.

Thus a mission definition phase includes these constraints in the development of a mission program.

1. Orientation of the Meter to the Flow Field:

In Section II of this summary report the analysis of the influence of the flow field and plasma sheath upon the electric field being measured is discussed. The significant aspect of this study was that the orientation of the meter must be such that the electron beam is in a plane perpendicular to the flow field. An allowable variation of $\pm 30^\circ$ from this position is computed, thereby reducing the attitude control requirement of the spacecraft to easily attainable limits.

This orientation assures that the wakes of the components of the meter do not intersect the beam, thereby maintaining the ambient electric field intensity along most of the path of the beam.

2. Location of the Electron Beam Relative to Physical Structures:

The electron beam field meter should be located at least 5 body radii from the spacecraft for ambient field measurements to assure that the electric fields associated with the plasma sheath about the craft do not distort the ambient field. However, when plasma sheath field measurements are being made the device is located as close as possible to the surface of the spacecraft.

The Faraday cage which surrounds the electron beam is located 10 cm from the electron beam. The wire composing the cage is 0.05 mm in radius. Thus the beam is located in excess of 1000 wire radii away from the cage. Negligible field distortion will result due to the introduction of the Faraday cage, providing that the orientation of the device to the flow field is maintained.

3. Meter Measure Two Orthogonal Components of the Electric Field:

Since the forces produced by electric field components along the electron beam do not produce beam deflection, the device responds to only two of the three components of the electric field vector.

Thus to measure all three components of the electric field, two possibilities exist:

- (a) Use two meters, orthogonal to each other, and located in the plane perpendicular to the flow field.
- (b) Rotate the vehicle, using one meter which lies in the plane perpendicular to the flow field.

The use of the two meters permits redundancy in the measurement of the electric field component parallel to the flow field, thus permitting correlation of readings.

4. Outgassing, Secondary Emission and Photoemission Effects:

During the mission various phenomena will change the ambient properties of the ionosphere. Three of these are:

- Outgassing
- Secondary Emission
- Photoemission for surfaces.

Each of these must be considered to assure proper design of the meter and interpretation of the measurement.

a. Outgassing

The efflux of waste material and gases will raise the ambient pressure in the vicinity of the vehicle. An electron beam traversing a region of increased pressure will experience additional collisions. These collisions will cause an attenuation of the beam electron density by scattering. Since the number of ion pairs produced is directly related to the beam current, the use of a one microampere or less beam assures that the number of ion pairs produced is not excessive for reasonable pressure rises. It would be advantageous to raise the acceleration potential of the electron gun, as this would also reduce the ions produced; however, as the beam voltage rises, the beam is less sensitive to the electric field. A parametric study indicated that an operation voltage between 300-500 volts would optimize the device. Table I illustrates the electron beam influence upon the environment as the pressure of the environment varies. (30, 31, 33)

b. Secondary Emission

The electron beam striking the collecting plate creates secondary emission of electrons, which would cause the ambient electron density to rise if they were allowed to escape. In addition, the secondary electrons effectively reduce the current being used to drive the nulling loop.

Thus, a screen mesh located close to the target with a repelling voltage of 90 volts, assures that most of the secondaries return to the target. Thus, the ambient electron density is not appreciably changed and sufficient current is available to drive the loop.

c. Photoemission and Charge Particle Fluxes

Various mechanisms exist in the ionosphere for the production of charged particle fluxes. Thus in the design of the instrument it was necessary to

Table I: Electron Beam Influence Upon the Environment

Neutral Environment			N #ion/cm-sec.	n e/cc			J amperes/cm ²		
$\frac{\#}{n_o \text{ cc}}$	Alt. Equiv. n_e ambient	Pressure at 300°K mm of Hg		r = 1 cm	r = 10 cm	r = 100 cm	r = 1 cm	r = 10 cm	r = 100 cm
3×10^{11}		10^{-5}	6.25×10^9	5×10^4	5×10^3	5×10^2	10^{-10}	10^{-11}	10^{-12}
3×10^{10}	200 km 10^5 e/cc	10^{-6}	6.25×10^8	5×10^3	5×10^2	5×10^1	10^{-11}	10^{-12}	10^{-13}
3×10^9	300 km 10^6 e/cc	10^{-7}	6.25×10^7	5×10^2	5×10^1	5	10^{-12}	10^{-13}	10^{-14}
3×10^8	400 km 5×10^5 e/cc	10^{-8}	6.25×10^6	5×10^1	5	5×10^{-1}	10^{-13}	10^{-14}	10^{-15}
3×10^7	600 km 10^5 e/cc	10^{-9}	6.25×10^5	5	5×10^{-1}	5×10^{-2}	10^{-14}	10^{-15}	10^{-16}

allow for the change of the ambient flux density which is distributed uniformly across the surface of the segmented collector plate. The technique of measuring the differential current caused by the deflection of a less than 1 mm diameter electron beam which is continually nulled to the center of the target plate, permits fluxes of greater than 10 microamperes to occur without saturating the differential amplifier. Whipple⁽³²⁾ reports that characteristic photoemission current density is about a nanoampere per square centimeter. A target plate of one square cm would have a negligible current rise due to incident flux, permitting the differential amplifier to operate normally.

d. EMI and RFI

There are two aspects of EMI and RFI; (1) that which is produced by the device, (2) that which is produced by the environment which limits the usefulness of the device.

(1) EMI and RFI of the Device

Considering each component separately, it is possible to establish the devices EM or RF produced environment.

(a) Electron Gun

The electron gun has a directly heated filament which for the laboratory model is pure tungsten. It uses D.C. current of 3.6 amperes and voltage of 3 volts. The filament lead wires are twisted, thus magnetic fields are cancelled.

The accelerating potential is 500 volts D.C. and the focussing screen potential is 120 volts D.C. The electrostatic shielding of the gun structure eliminates static electric field from the environment.

The electron beam is less than one microampere and travels 18 cm to the target. The magnetic field produced is approximately:

$$B = \mu_0 I / 2 \pi r \quad \text{weber/m}^2$$

where $r = 5 \times 10^{-4}$ meters
 $I = 10^{-6}$ amperes
 $\mu_0 = 4\pi \times 10^{-7}$ henry/meter

Thus, the magnetic field produced by the beam at its surface is approximately 10^{-10} webers/meter².

The chopper is electromechanical and thus has a small noise EMI spectrum about its 400 cps rate. This power spectrum will be insignificant after encasing within the read-out chassis.

(2) EMI and RFI of the Environment

Since the device is designed to measure electric fields both static and slowly varying, externally produced electric or magnetic fields would disturb its readings. However, since the measurements are highly filtered around the chopping frequency, rapidly varying fields will be discriminated against. Magnetic fields of any nature are discriminated against by the operation of the Faraday cage.

Elimination of the disturbance of static or slowly varying electric field is obtained by either physical separation or orientation of the device with respect to the source. A constant background electric field can be normalized out of the measurements.

D. ATTITUDE RESOLUTION REQUIREMENTS

Since the electric field meter is located aboard a spacecraft moving relative to the magnetosphere the electric field measured by the meter exists only in the reference frame moving with it.⁽³⁴⁾ It is therefore necessary to transform this field to a frame fixed relative to the earth, since this is the ambient electric field within the ionosphere.

In order to accomplish this transformation it is necessary that the following be measured:

- Vector ambient magnetic field relative to the spacecraft,
- Velocity of the spacecraft relative to the earth,
- Attitude of the spacecraft relative to the frame of reference fixed to the earth.

1. Requirements for Resolution of Attitude Measurements:

The velocity vector of an orbiting vehicle can be determined to better than one part in 10^5 by ground tracking. However, it is necessary to know the attitude of the vehicle relative to the inertial frame to use this velocity measurement in computing the $(\bar{v}_s \times \bar{B})$ field acting on the vehicle. The local magnetic fields are measured by on-board three axis magnetometers. The velocity vector can be related to the satellite reference frame using the attitude measurements. In this frame the electric field measurement is made.

We can examine the requirement upon the attitude measuring system for a given error in the determination of the $(\bar{v}_s \times \bar{B})$ field. This component of the measured electric field consists of the following terms:

$$\bar{e} + \Delta \bar{e} = (\bar{v}_s \times \bar{B}) + (\bar{v}_s \times \Delta \bar{B}) + (\Delta \bar{v}_s \times \bar{B}) + (\Delta \bar{v}_s \times \Delta \bar{B})$$

where

$\Delta \bar{B}$ is the error in the measurement of B

$\Delta \bar{v}_s$ is the error in the velocity due to the error in measurement of the vehicle attitude.

The error terms can be examined separately, and the last term on the right hand side can be neglected because of smallness. Thus the error is:

$$\Delta \bar{e} = (\bar{v}_s \times \Delta \bar{B}) + (\Delta \bar{v}_s \times \bar{B})$$

The maximum error occurs when $\Delta \bar{B}$ is perpendicular to \bar{v}_s and $\Delta \bar{v}_s$ is perpendicular to B simultaneously. From this the $|\Delta \bar{v}|$ error can be related to the other terms as:

$$|\Delta v_g| = \frac{|\Delta e| - |v_g \Delta B|}{|B|} \quad \text{meters/second}$$

and the attitude measurement error permissible is:

$$\Delta \theta = \frac{|\Delta v|}{|v|} \quad \text{milliradian.}$$

Table II lists the required attitude accuracy in radians of arc for orbital velocity of 7.5×10^3 meter/second upon assumed errors in measuring the magnetic field and desired accuracy of determining the $(v_g \times B)$ field. This is based on the maximum error, thus the accuracy of $(v_g \times B)$ will be better most of the time. The maximum magnetic field is assumed to be 0.4 gauss (4×10^{-5} webers/m²).

TABLE II
Required Attitude Resolution (in radians)

ΔB milligauss Δe (millivolts/meter)	0.5	1	2.5	5
0.4	0.88	----	----	----
0.8	1.4	0.17	----	----
2.0	5.4	4.2	0.8	----
4.0	12.0	10.8	7.5	0.8
8.0	26.0	24.0	21.0	14.0

This table shows the most severe requirements on the attitude measuring system. It shows the range from the most precise measurement of about 0.1 milliradian (roughly to within 20 seconds of arc) to a rather crude measurement of 25 milliradians (roughly 1.5 degrees of arc). Therefore system sensitivity can be estimated based upon the accuracy of the magnetometer measurements, resolution of the attitude measurement, and the acceptable error in the $(v_g \times B)$ determination.

2. Component of Electric Field Parallel to the Magnetic Field:

It is possible to determine the component of the electric field which is parallel to the magnetic field without knowledge of the spacecraft attitude in an inertial frame of reference. The two aspects of this technique which reduce its value are:

- (a) Since the conductivity of the ionosphere is anisotropic, the electric field sustained parallel to the magnetic field is in the order of 100 times less than the electric field perpendicular to the magnetic field.
- (b) Knowledge of the parallel and perpendicular components of the electric field do not completely define the field orientation.

However, for completeness the following analysis is included:

$$\vec{M} = \vec{E} + \vec{v} \times \vec{B} \quad (1)$$

where \vec{M} is the electric field as measured by the instrument (V/m)
 \vec{E} is the ambient electric field (V/m)
 \vec{B} is the local magnetic field (web/m²)
 \vec{v} is the vehicle velocity (meters/sec)

The apparent electric field due to the electron velocity relative to the magnetic field is eliminated by the Faraday cage technique used with this instrument described in Section III of this report.

Now if the scalar product is taken with the magnetic field and the measured electric field we have:

$$\vec{B} \cdot \vec{M} = \vec{B} \cdot \vec{E} + \vec{B} \cdot (\vec{v} \times \vec{B}) \quad (2)$$

since, $\vec{B} \cdot (\vec{v} \times \vec{B}) = 0$,
 $\vec{B} \cdot \vec{M} = \vec{B} \cdot \vec{E}$

Thus,

$$E_{\parallel} = \frac{\vec{E} \cdot \vec{B}}{|\vec{B}|} = \frac{\vec{M} \cdot \vec{B}}{|\vec{B}|} \quad (3)$$

where E_{\parallel} is the electric field component parallel to the magnetic field.

In terms of the three directional field components $M_1 M_2 M_3$ (measured in a + llite fixed coordinate system) and of the three field components $B_1 B_2 B_3$ measured by magnetometers directed along the same vehicle axes, one obtains for Equation (3):

$$E_{11} = \frac{M_1 B_1 + M_2 B_2 + M_3 B_3}{(B_1^2 + B_2^2 + B_3^2)^{1/2}} \quad (4)$$

Thus, E_{11} can be measured without recourse to measurement of velocity V or of vehicle attitude angles.

An error analysis of Equation (4) has been made. Table III gives typical results of the accuracy of E_{11} (in millivolts/meter) based upon assumed errors in individual measurements M and magnetic field measurement errors. Thus, if each component of M is measurable to 1 mv/meter the parallel field E_{11} may be calculated to the same accuracy if magnetic components are known to 0.5 milligauss (50 gamma) or better.

TABLE III
Error in E_{11} (millivolts/meter)

Error in individual component of M , millivolts/meter	Error in B (milligauss)	0.5	1	2.5	5.0
	0.4	0.53	0.81	1.81	3.56
	0.8	0.87	1.07	1.94	3.62
	2.0	2.0	2.12	2.67	4.06
	4.0	4.0	4.06	4.36	5.34
	8.0	8.0	8.03	8.2	8.75

3. Magnetic Field Measurement Requirements:

Whenever the error due to the vehicle motion is excessive with respect to the electric field being measured, it is necessary not only to know the vehicle velocity and attitude, but also the magnetic field.

Thus, a three axis fluxgate magnetometer is a necessary associative meter to fully reduce the data collected by any electric field meter on an orbiting spacecraft moving relative to the magnetosphere.

The fluxgate magnetometer responds to all magnetic fields. Internal magnetic fields generated aboard the spacecraft decay as the inverse cube of the ratio of the distance to the meter and the radius of the spacecraft. Thus a magnetometer located 5 body radii from the spacecraft, permits internal magnetic fields which leak out to be as large as 0.5 gauss without jeopardization of the measurement of the ambient magnetic field for orbits between 200 and 2000 km altitude.

A three axis fluxgate magnetometer can be calibrated to have a precision of 1 milligauss for magnetic fields as large as 0.5 gauss. Its physical size is a cylindrical sensor of 50 cu. inches and an auxiliary power and read-out package of 75 cu. inches. Its total mass is 3 pounds.

4. Attitude Resolution Requirements for Specific Missions:

Since the magnitude of the electric field varies with each mission, the degree to which the attitude must be known also varies.

Assuming that the magnetic field components are each measured to an accuracy of 1 milligauss, the velocity of the vehicle relative to the earth is measured to better than one part in 10^5 , and the orbit lies between 200-2000 km; it is then possible to assess the required attitude resolution requirements for the mission.

a. Category I - Engineering or Housekeeping

(1) Charged Contaminant Cloud Electric Fields

Since the range for this field is extremely wide (10^{-2} to 10^2 volts/meter) which reflects our lack of knowledge of the phenomena, the range of attitude resolution is likewise wide.

To maintain an error less than 10% of the expected field value, the attitude resolution necessary to measure the minimum field expected is 40 seconds of arc, while the attitude resolution requirement for the largest field is in excess of 90° with errors less than 1% expected.

This range of attitude requirements from 40 seconds to over 90° indicates that with improved knowledge of the phenomena better predictions of attitude resolution accuracy will be obtained. These may well prove to present no problems to typical manned spacecraft systems.

(2) Sheath Interaction Electric Field

Since these fields are typically reasonably strong (from 10^0 to 10^2 volt/meter), the attitude resolution requirements are essentially non-existent. They range from 1.5° to over 90° of arc for less than 1% error in measurement.

(3) Forces and Moments Due to Ionospheric Electric Fields

For this mission two electric fields must be measured; the surface and the ambient electric field. Attitude resolution for surface field measurements were given in (2) above, while the range of ambient electric field values (from 10^{-2} to 10^0 volts/meter) requires high precision of attitude resolution.

For ambient electric field attitude resolution requirement is for 40 seconds of arc for an error of 10% for the minimum field and 1% or better for the maximum field.

(4) Lunar Environment

Since the magnetic field in the lunar environment is significantly smaller than near earth, and since the range of electric fields (10^{-1} - 10^3 volts/meter) indicate relatively strong fields, it is doubted that the $(\vec{v} \times \vec{B})$ contribution will represent a significant problem.

b. Category II - Scientific or Survey Missions

(1) Ambient Electric Field

The attitude requirement of 40 seconds of arc was discussed previously. This would assure an error less than 10% at the minimum field value and less than 1% at the maximum field value.

(2) Sounding Rockets

The use of the near vertical trajectory in the polar regions minimizes the $(\vec{v} \times \vec{B})$ problem when measuring the ambient electric field. The two reasons are:

- The vertical trajectory nearly cancels the $(\vec{v} \times \vec{B})$ contributions to the measurements of the ascending and descending legs.
- The magnitude of the $(\vec{v} \times \vec{B})$ contribution is small due to the low velocity and small angle between these vectors.

5. Summary of $(\vec{v} \times \vec{B})$ Problem:

This discussion presented in this section was intended to point out a problem inherent with all electric field meters located aboard a spacecraft moving relative to the magnetosphere. The extent of the problem depends upon:

- The range of electric field values to be measured,
- The trajectory of the vehicle,
- The velocity of the vehicle,
- The precision to which the measurement must be made.

The accuracy of 40 seconds of arc indicated as the most severe requirement, is actually a greater restraint than will normally be required. This resolution requirement was derived for the case where the error in the velocity measurement was perpendicular to the error in the magnetic field measurement. This situation is extremely rare, and a minimum resolution requirement would more realistically lie between 1 and 2 minutes of arc.

Attitude resolution to this degree will be available on most AAP missions. Another means of achieving this data would be by photographing the star fields during the measurement operation and later determining the attitude at the time of measurements.

E. MISSION CONFIGURATIONS

Although there are many possible configurations we will consider two which encompass most of the missions:

- Multipurpose Mission aboard AAP workshop
- Sounding Rocket Ballistic Mission.

1. Multipurpose Mission:

The choice of the AAP workshop as the spacecraft was based upon the following:

- Orbits exist between 200-2000 km.
- Attitude Resolution capabilities are excellent.
- Possibility of Astronaut operation of device.
- Surface extent sufficient for meaningful surface field measurements.
- Payload capacity.
- Optical charged cloud problem will probably exist.
- Many electromagnetic experiments will be performed modifying or being modified by the plasma sheath.
- Correlation of ambient electric field changes before, during, and after solar flares.
- Extensive duration missions, providing an excellent survey of the electric field under many conditions. In addition, electrodynamical drag and moments will have sufficient time to accumulate to be significant.

a. Concept of Mission

Since there are many possible objectives for the electric field measurements, and many common attributes, the concept of a few meters at appropriate and variable locations which sequentially are used for different measurements has been adopted.

The minimum number of meters and their locations are as follows:

- One - surface electric field meter, electron beam oriented perpendicular to flow, located downstream from most EM experiments.
- Two - electric field meters mounted on extensible booms variable distance from surface to 5 body radii, electron beam oriented perpendicular to flow and orthogonal to each other.
- One - three axis fluxgate magnetometer mounted on boom 5 body radii in length.

The sequencing of measurements will permit time sharing of the limited number of meters available. Normal operation will have a duration of two minutes, and the frequency will be four times an orbit.

<u>Mission</u>	<u>Meters Required</u>	<u>Expected Measured Values</u>
Category I		
a. Charged cloud fields	1, 2, 3	10^{-2} to 10^2 volts/meter
b. Plasma sheath field	1	10^0 to 10^3 volts/meter
c. Forces and moments	1, 2, 3	10^{-2} to 10^3 volts/meter
	(magnetic field (3))	(10^{-2} to 5×10^{-1} gauss)
Category II		
a. Survey	2, 3	10^{-2} to 10^0 volts/meter

where: meter 1 is the surface electric field meter,
meter 2 is the extensible boom mounted electric field meters,
meter 3 is the boom mounted magnetometer.

Each meter will normally operate 8 minutes per orbit. The life expectancy of the filament is over 500 hours; thus roughly 4,000 orbits or about 8 months operation can be expected from each meter. This will be reduced if the meters are placed in continuous operation mode to observe a charged cloud formation or dissipation; or to observe events for longer than two minutes during a solar flare.

The output of the meters will be a d. c. voltage (0. - 5 volts) suitable for either telemetry or recording or both. Each electric field meter requires 4 data read-out channels and 20 housekeeping channels; the magnetic field meter requires 4 data and 10 housekeeping channels. This is a preliminary estimate requiring about 90 channels when all meters are operative. During the experiment definition phase, redundancy will be eliminated and time sharing of channels will be considered, based upon the number of channels available for telemetry. Since the data can be read out after the measurement, the number of channels can be reduced to fit any specific flight mission plan. Standard IRIG telemetry sampling rates will be used and time standard will be the spacecraft clock.

b. Physical and Electrical Configuration

The spacecraft being considered is the AAP workshop whose body radius is about 3 meters and length about 15 meters. Thus the 5 body radii extensible boom has a maximum length of 15 meters. This boom will support either an electric field meter sensing head having a mass of one pound (this unit was shown in Figure 1) or a magnetometer head, also weighing one pound in cylindrical shape - 3 inches in diameter and 6 inches long. A design study to be conducted during the experiment definition phase will finalize the extensible control mechanism, the stresses allowable for the boom, and its load carrying capacity. A cable harness will connect the sensing heads of the meters to their respective housekeeping packages located within the spacecraft. The electric field housekeeping unit will have a mass of 2 pounds, cylindrical shape of 6 inch diameter, 6 inch length. The magnetometer housekeeping unit has a mass of 2 pounds, and cylindrical shape of 3 inches diameter and 10 inches in length. The total cable mass for each extensible harness is estimated at 5 pounds and the booms' mass is estimated at 10 pounds. The boom storage container will be a cylinder of 1 foot diameter and 0.8 feet wide. The booms will extend up to 15 meters in length and be 2 inches in diameter. The total payload mass is estimated as follows:

<u>Unit</u>	<u>Quantity</u>	<u>Total Mass pounds (kg)</u>	
Electric Field Sensing Heads	3	3 (1.361)	3 (1.36)
Magnetometer Sensing Head	1	1 (0.454)	1 (0.454)
Electric Field Housekeeping Package	3 (if simultaneous)	6 (2.71)	-
	1 (if sequential)	-	2 (0.905)
Magnetometer Housekeeping Package	1	2 (0.905)	2 (0.905)
Extensible Boom Package	2 (if two E meters on same boom)		20 (9.05)
	3	30 (13.6)	-
Cable Harness	3	15 (6.6)	15 (6.6)
		max. 57 (25.8) min. 43 (19.4)	

() System International units (kilograms)

Therefore a total payload weight between 43 to 57 pounds is estimated for the experiment.

The electrical power is assumed to be available from the space-craft prime power, and only signal conditioning is included in the mass estimate. The housekeeping units will draw the power for the meter operations, and the boom extension package will draw the power during erecting and length variation procedure. The power drain is estimated as:

<u>Unit</u>	<u>Quantity</u>	<u>Stand-by</u>	<u>Average</u>	<u>Maximum (watts)</u>
Electric Field Meter	3	6	36	45
Magnetometer	1	1	1	2
Boom	3	0	1.5	3
Total Power Requirements		7	38.5	50 watts

This power estimate is based upon a tungsten filament, which is being used in the laboratory breadboard. The total power requirement can be reduced by as much as 10 watts per electric field meter if oxide coated filaments are used. This would reduce the payload power requirements to:

<u>Power Requirements</u>	<u>Stand-by</u>	<u>Average</u>	<u>Maximum (watts)</u>
Payload total	2	8.5	20

In summary the flight package including 3 electric field meters, 1 magnetometer, 2 or 3 booms with housekeeping and harnesses is estimated to have a mass of 43 to 57 pounds and an electrical requirement of 2 watts standby, 8.5 watts to 20 watts for operation. The conceptual sketch of the multi-purpose mission is shown in Figure 11.

2. Sounding Rocket Ballistic Mission:

These flights provide a means of measuring the ambient electric fields during solar flares or auroral displays. Two ballistic launches of sounding rockets would be desirable. Since the magnetic field flux tubes terminate in the polar regions, a launch site such as Fort Churchill would be preferred. One launch will be accomplished during a quiet solar period and the other during active solar periods. A near vertical launch would permit the near cancellation of the $(\vec{v}_s \times \vec{B})$ electric field, thus the vehicle attitude and velocity need be known to moderate accuracy. The ambient vector electric and magnetic field, and the plasma to vehicle potential differences will be measured. The apogee will be in the order of 2000 km, and data will be telemetered to ground stations negating the need for recovery. The vehicle would be spin stabilized, thus only one electric field meter is required for the three components of the electric field.

The meter, aligned as shown in Figure 12 , will present minimum plasma sheath interference due to the component parts of the meter. The ambient electric field meter will be mounted on a folded boom which would extend at an altitude of 100-200 km and remain extended to re-entry. A symmetrical boom would house the three axis magnetometer. All systems would operate continuously from time of boom extension to re-entry. Data will be processed within the house-keeping payload and telemetered from the vehicle. Ground radars will track the payload throughout the flight.

a. Ballistic Flight Considerations

A near vertical launch in the polar region would reduce the magnitude of the $(\vec{v}_s \times \vec{B})$ field which perturbs the electron beam electric field measurement. In addition the symmetry of the ascent and descent of the payload permits approximate cancellation of the perturbing field from the data. However,

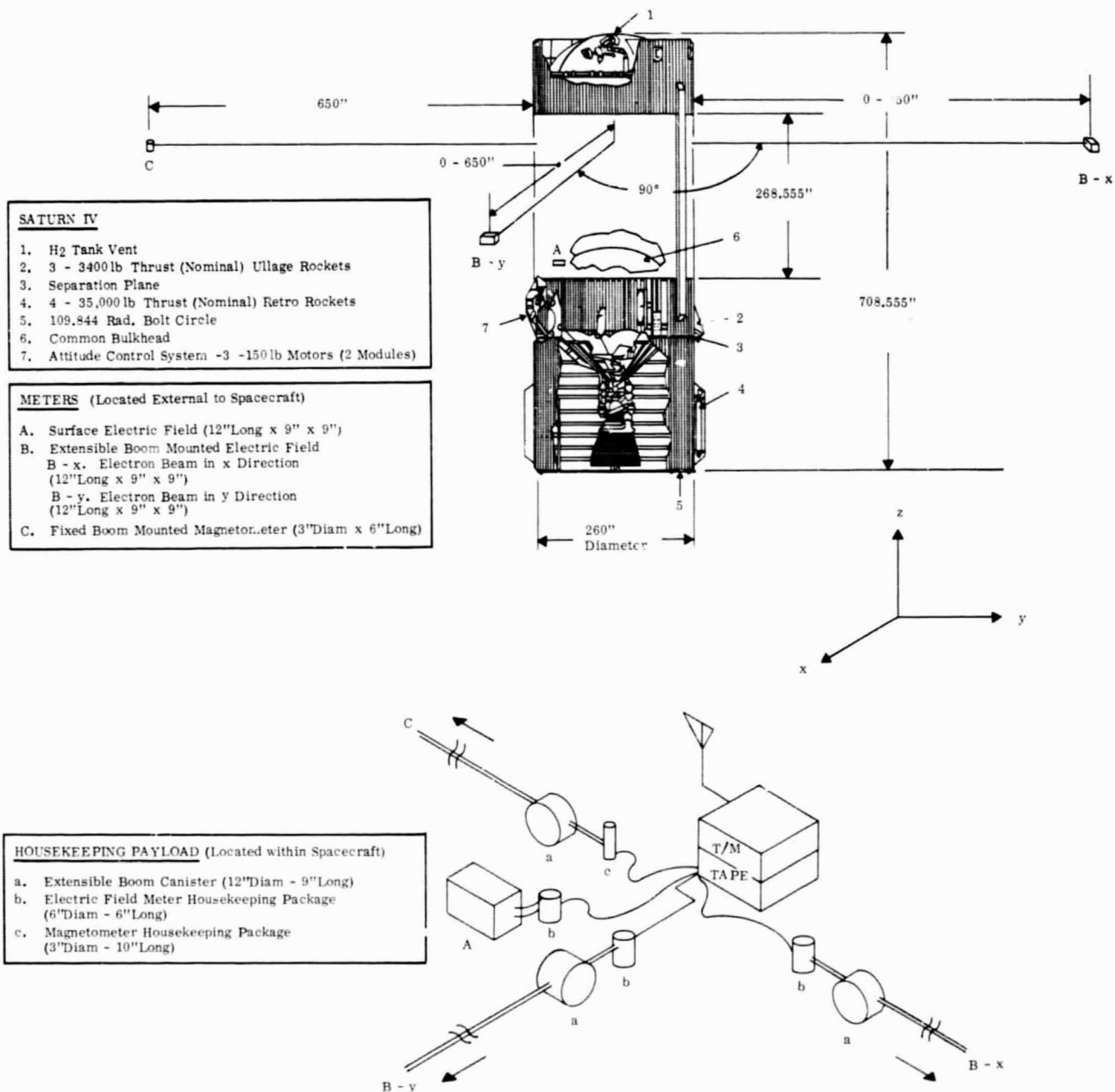


Figure 11: AAP Workshop Conceptual Configuration

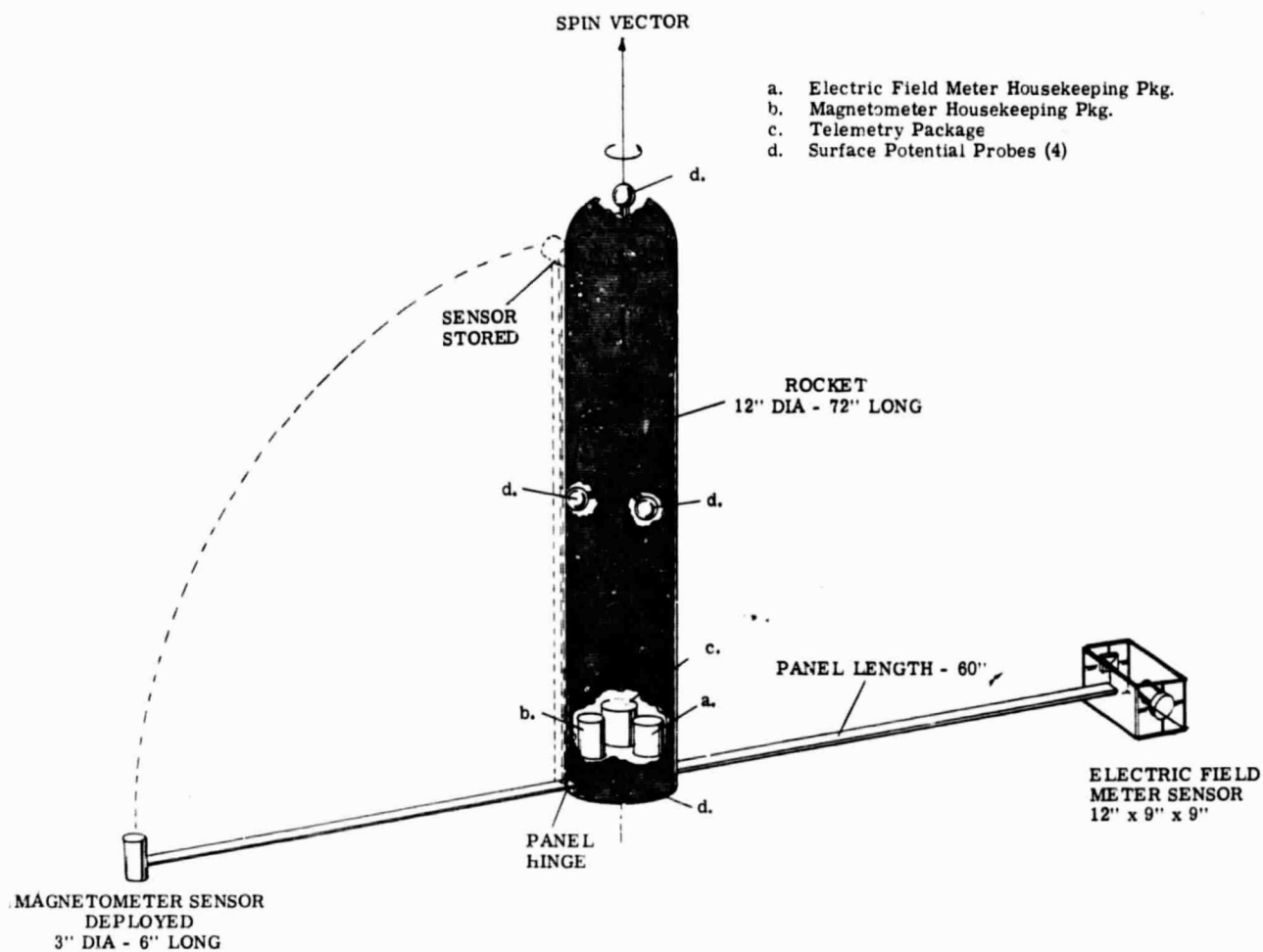


Figure 12: Sounding Rocket Conceptual Configuration

to assure knowledge of the magnetic field vector during the flight it is recommended that a three axis fluxgate magnetometer, capable of resolving each magnetic field component to an accuracy of 1 milligauss, be mounted on a symmetrical folded boom to the electric field meter. The boom length would be about 5 feet depending upon the structural constraints of the payload. This distance assures the decay of the vehicle plasma sheath electric field to less than 1 millivolt/meter at the meter providing the meter is not in the vehicle wake, and requires the internal magnetic field of the vehicle to be less than one gauss for 1/2 foot radius housekeeping payload. The internal magnetic field is minimized by choice of materials, and placement of current carrying wires.

Spin stabilization is recommended as the simplest method to maintain attitude during the flight. However, the spin rate chosen must represent a compromise between the electron beam Faraday cage chopping rate, the number of E field samples per measurement integration, the time variation of the nutation of the payload, and the number of degrees rotation smear per measurement. For example, a spin rate of 10 r.p.m. would permit 30 samples at a 400 cps chopping rate and a vehicle rotation of 5 degrees during integration.

Since the most important data is the ambient electric field vector relative to the magnetic field vector, precise knowledge of vehicle attitude at the time of measurement is not required. The modulation of the telemetered data due to vehicle nutation would provide sufficient attitude information for data reduction.

The electron beam for the ambient electric field meter will be fired in a direction perpendicular to the velocity vector. Providing that nutation angle is less than 30° , this orientation will assure that the beam is not in the wake of the components of the meter. If we let the velocity lie along the z axis, then the beam is in the x-y plane. Thus during rotation the components E_z and E_x and then E_z and E_y are alternately measured every 90° of rotation. By sampling every 5° it is possible to reconstruct the electric field vector during the measurement. The altitude change during each 5° measurement is about 1000 feet, decreasing as it nears the apogee. Electrostatic surface potentiometers will be placed at various locations on the payload to monitor the surface field changes. Due to the probable size of the

housekeeping payload for the ballistic flight, it is doubtful that a surface field meter would be appropriate for this test.

b. Physical and Electrical Configurations

For this mission one electric field meter and one magnetometer with associated housekeeping packages, as well as two five foot booms with two cable harnesses and prime power batteries is required.

The mass estimate is:

Electric Field Sensor Head	1 pound	(0.4536 kg)
Electric Field Housekeeping Package	2 pounds	(0.906)
Magnetometer Sensor Head	1 pound	(0.4536)
Magnetometer Housekeeping Package	2 pounds	(0.906)
Harnesses (two)	2 pounds	(0.906)
Boom (two)	6 pounds	(2.72)
Batteries and mounts	10 pounds	(4.536)
Telemetry Transmitter	<u>6 pounds</u>	<u>(2.72)</u>
Total Payload Weight:	30 pounds	(13.6)
() System International Units (kg)		

The electric power requirement is 12 watts for 30 minutes or 6 watt-hours.

F. IN-FLIGHT ELECTRIC FIELD METER OPERATION

After boom extension, the filament is allowed 1/2 minute warm-up prior to the application of the gun voltages. The amplifiers are normally in stand-by operation maintaining temperature and voltage stability. The electromechanical chopper is activated when filaments are being warmed-up. When the electron gun is fully operational, the Faraday cage is shorted (zero electric field), the electron beam is centered by the nulling voltages on the two axis deflection plates. The zero electric field voltage is recorded along with spacecraft time and attitude data. Then the sequencing of the chopped field calibration is started. The synchronous detector provides a d.c. voltage proportional to the electric field which is chopped by the

intermittent application of the Faraday cage. The calibration of electric field versus output voltage will be initially performed on the ground. In flight calibration is accomplished by applying stepped known voltages at the chopping rate to the Faraday cage plates when they are not shorted together and recording the nulling voltages. After calibration, the normal operative mode occurs; the external electric field to be measured is chopped by the action of the Faraday cage and the d.c. output voltage of the two axis are stored for telemetry or recovery. The form of the output will be a 0-5 volt signal which can be used in standard telemetry.

A typical operation procedure is given below:

Typical Operation Procedure

1. Stand-by condition, amplifiers warm and stable,
2. Boom extension
3. Filament warm-up (1/2 minute); electromechanical chopper operative,
4. Gun voltages applied,
5. Faraday cage shorted (zero field calibration) d.c. output voltage of demodulator-filter is stored.
6. Faraday cage opened (electric field calibration), chopped voltages applied to two axis Faraday plates in turn, d.c. output and applied input voltages are stored for calibration to update ground calibration.
7. Normal chopped mode, Faraday cage is alternately created and removed, the d.c. output voltage of the demodulator-filter is stored.

In addition to the d.c. output voltage, the time of measurement, the attitude of the vehicle and the vector magnetic field are required to interpret the electric field measurements. These data must be telemetered with each reading.

PRECEDING PAGE BLANK NOT FILMED

REFERENCES

1. O'Brien, Brian, J., "The Magnetosphere and Auroras", Astronautics and Aeronautics, July, 1967, pp. 16-26.
2. Wildman, P.J.C., "A Device for Measuring Electric Fields in the Presence of Ionization", Jour. of Atom. and Terr. Physics, V. 127, No. 3, 417 (1965).
3. Kavadas, A., and Johnson, D.W., "Electron Densities and Electric Fields in the Aurora", Space Research IV, North Holland Publishing Co., 1964 p. 365.
4. Haerendel, G. Report of an electric field measurement using neutral gas and ionized barium clouds presented at the ESRO Conference in Stockholm, Sweden 1965.
5. Fahleson, U., "Theory for Electric Field Measurements in the Magnetosphere with Electric Probes," Royal Inst. of Tech., Sweden, Report 66-02, Feb. 1966.
6. Shriver, E.L., "Investigation of the Deflection of an Electron Beam as a Means of Measuring Electric Field Strength," MSFC, NASA TX-53435, April, 1966.
7. Ya. L. Alpert, A.V. Gurevich and L.P. Pitaevski, "Space Physics with Artificial Satellites," Consultants Bureau, New York (1965).
8. Kum-Min Chen in "Interactions of Space Vehicles with an Ionized Atmosphere," edited by S. F. Singer, p. 465, Pergamon Press (1965).
9. Pung Nien Hu and Sigi Ziering, Phys. of Fluids, Vol. 9, No. 11, p. 2168 (1966).
10. Lee W. Parker, NASA Contractor Report, NASA CR 618, October, 1966, also CR 401, March, 1966.
11. G.L. Gdalevich and I.M. Imyanitov, in NASA Technical Translation, NASA TT F 389, p. 367, (1966).
12. McPherson, D.G., "ATM Contamination Study," NASA CR 61173, May, 1967.
13. F.T.F. Osborne, F.H.C. Smith, R.E., Barrington and Mather, W.E., "Plasma Induced Interference in Satellite v.l.f. Receivers," Canadian Jour. of Physics, Vol. 45, (1967) p. 47-56.

14. F. W. Crawford, R.S. Harp, and Mantel, T.D., "Pulsed Transmission and Ringing Phenomena in a Warm Magnetoplasma," IEEE, International Antennae and Propagation Symposium, 1966, Palo Alto, California.
15. F. W. Crawford and R. J. Harp, J. Geophy. Research, 70, 587 (1965).
16. Cook, G.E., "On the Accuracy of Measured Values of Upper-Atmosphere Density," JGR, Vol. 70, No. 13, (July, 1965).
17. Bryant, R., "Densities Obtained from Drag on the Explorer 17 Satellite," JGR., 69, (1964).
18. Newton, G.P., R. Horowitz, and W. Priester, "Atmospheric Density and Temperature Variations from Explorer 7 Satellite and Further Comparison with Satellite Drag," Planet, Space Sci., Vol. 13, p. 599-616 (1965).
19. Friedman, M.P., "A Critical Survey of Upper Atmosphere Density Measurements by Means of Ionization Gauges," Smithsonian Institution Astrophysical Observatory, Report No. 217, (July, 1966).
20. Nigam, R.C., "Effect of Atmospheric Oblateness on the Acceleration of Satellite," J.G.R., Vol. 69, No. 7, p 1361 (1964).
21. Drell, S.D., H.M. Foley, and M.A. Ruderman, "Drag and Propulsion of Large Satellites in the Ionosphere," J.G.R., Vol. 70, No. 13, p. 3131 (1965).
22. Groves, G.V., "Atmospheric Densities Obtained from Satellite Orbits," Proc. of the First International Symposium on Rocket and Satellite Meteorology, p. 422-436, John Wiley & Sons, Inc., New York (1963).
23. Axford, W.L., and C.O. Hines, "A Unifying Theory of High Latitude Geophysical Phenomena and Geomagnetic Storms," Can. J. Phys., 39, p. 1433 (1961).
24. Megil, L.R., and N.P. Carleton, "Excitation by Local Electric Fields in the Aurora and Airglow," J. of Geoph. Res., Vol. 69, p 101 (Jan, 1964).
25. Bostrom, R., "Model of the Auroral Electrojets," J. Geophys. Res., 69, p. 4983-4999 (1964).

26. Atkinson, G., "Polar Magnetic Substorms," J. of Geophys. Res., Vol. 72, p. 1491, March 1967.
27. Manual on Rockets and Satellites, Berkner, L.V., Editor, Vol. VI, p.164-168, Pergamon Press (1958).
28. Gurevich, A.V., and A.M. Moskalenko, "Braking of Bodies Moving in a Rarefield Plasma," Space Res., NASA TT F 389, p.322-341, (May, 1966).
29. M. Petschek, "Surface Electric Field Measurement," NASA SP-88, NASA Summer Conference on Lunar Exploration and Science, Falmouth, Mass. (1965).
30. Markevitch, B.W., and F.C. Hurlbut, "The Study of Electron Beam Attenuation in Air," University of California Report TR HE 150-142, (February, 1957).
31. Spangenberg, K.R., Vacuum Tubes, McGraw Hill, New York (1948).
32. Whipple, Jr., E.C., "The Equilibrium Electric Potential of a Body in the Upper Atmosphere and in Interplanetary Space," NASA TMX-55368, Goddard Space Flight Center, (June 6, 1965).
33. Massey and Burhop, Electronic and Ionic Impact Phenomena, Clarendon Press, (1956).
34. F.J.F. Osborne and M.A. Kasha, "The $v \times B$ Interaction of a Satellite with its Environment," Canadian Jour. of Physics, Vol. 45, 1, 263-277, (1967).